4. $\delta^{13}C_{CO3}$ AND $\delta^{18}O_{CO3}$ SEAWATER PROFILES THROUGH THE PERMIAN-TRIASSIC OF AUSTRALASIA

4.1 Introduction

An attempt to define the $\delta^{13}C_{CO3}$ and $\delta^{18}O_{CO3}$ seawater profiles through the Permian-Triassic boundary of Australasia was unsuccessful because no marine carbonate sections are known (Morante, 1993). The sedimentary basin with the section with the richest carbonate material is the Bowen Basin, where Geological Survey of Queensland (GSQ) coreholes containing shelly faunas cover a time interval from Stage 3b to lower Upper Stage 5. Supplementary material from younger Permian and Triassic sediments was sought from outcrop in the Sydney Basin, the Australian northwest (Canning Basin), and New Zealand (Southland Geosyncline). The location of corehole sections sampled is listed in Table 2.0. The locations of outcrop samples are listed in Appendix 4.1 (Table 4.4).

4.2 Sample selection and screening

$\delta^{13}C_{CO3}$ values were determined on low-magnesium calcite from fabric-retentive non-luminescent brachiopod shells. Non-luminescent brachiopods are thought to have the maximum chance of preserving the original seawater $\delta^{13}C_{CO3}$ and $\delta^{18}O_{CO3}$ values (Popp et al., 1986a; Marshall, 1992; Al-Aasm and Veizer, 1982), although Rush and Chafetz (1990) question the reliability of this criteria to determine whether a primary isotope signature is always retained.

Where the samples came from core, $\delta^{13}C_{org}$ determinations were generally conducted on samples from the same stratigraphic horizon. This enables calculation of Δ, the difference between the $\delta^{13}C_{org}$ and $\delta^{13}C_{CO3}$ values at a particular time. Δ values much larger or smaller than -28.5‰ are thought to indicate alteration.

An additional guide to the level of diagenetic alteration of the brachiopod shells included analysis of the $^{87}Sr/^{86}Sr$ in selected samples (see Chapter 3). Ratios in accord with, or lower than, those on the global $^{87}Sr/^{86}Sr$ curve of Denison et al., (1994) for the estimated age assignment of the sample in the Late Permian were considered to have probably retained their original $^{87}Sr/^{86}Sr$ and hence to have suffered little if any diagenetic alteration. Samples with high $^{87}Sr/^{86}Sr$ were treated as suspect and carefully re-examined using the cathode luminescent microscope and Δ was checked as a guide to the retention of primary $\delta^{13}C_{CO3}$ and $\delta^{18}O_{CO3}$ values. A low $^{87}Sr/^{86}Sr$ in brachiopod shell material from a predominantly siliciclastic matrix generally indicates that limited chemical exchange has occurred between the calcite and external pore fluids (Brand, 1991). This is because $^{87}Sr/^{86}Sr$ in siliciclastic sediments would normally be expected to be higher than in limestones or calcite shells hence any ion exchange with fluids interacting with the host rock would result in higher $^{87}Sr/^{86}Sr$.

Another guide to the level of chemical exchange of stable isotopes during diagenesis involved comparison of the $\delta^{18}O_{CO3}$ values of individual samples. As any exchange of stable isotopes during diagenesis is more likely to affect the $\delta^{18}O_{CO3}$ than the $\delta^{13}C_{CO3}$ (Marshall, 1992; Hallam, 1994), $\delta^{18}O_{CO3}$ values that were much lower than samples immediately adjacent in a section (more than 2‰) were considered as suspect. $\delta^{13}C_{CO3}$ is less readily affected by isotope exchange during diagenesis because carbon from the carbonate dissolved in pore fluids is generally the greatest proportion of carbon in the pore fluids (Marshall, 1992). Exchange of carbon atoms from calcite samples with carbon in pore fluids during diagenesis in all but open systems of pore fluid exchange is therefore likely to result in only a minimum variation in $\delta^{13}C_{CO3}$. It is, however, possible that homogenisation of $\delta^{13}C_{CO3}$ values occurs during diagenesis and that this blunts any natural rapid or erratic $\delta^{13}C_{CO3}$ signature. An example of this might be the smooth curve through the Late Permian/EarlyTriassic section at Gartnerkofel, Austria (Holser et al., 1989; 1991) where the dolomitised, recrystallised carbonate whole rock samples show smooth transitions with only minor isotope variation between adjacent samples.

As a test that cathodo-luminescence does indicate alteration, the $\delta^{13}C_{CO3}$ and $\delta^{18}O_{CO3}$ values of low-magnesium calcite, subsamples from luminescent and non-luminescent areas of individual brachiopod shells were analysed (Table 4.1). In each case luminescent shell had more negative $\delta^{13}C_{CO3}$ and $\delta^{18}O_{CO3}$ values than nonluminescent shell and the "alteration" to more negative values was greater for $\delta^{18}O_{CO3}$ than for $\delta^{13}C_{CO3}$.

Table 4.1 Comparison between $\delta^{13}C_{CO3}$ and $\delta^{18}O_{CO3}$ values obtained from cathodoluminescent and noncathodoluminescent portions of brachiopod or bivalve shells.

Location	Depth m	δ^{13}C ‰ lum	δ^{13}C ‰ nonlum	δ^{18}O ‰ lum	δ^{18}O ‰ nonlum
Taroom 10	890.7	1.90	5.50	-5.92	-1.98
Taroom 10	897.2	4.42	6.96	-5.21	-1.19
Taroom 10	946.45	4.87	7.46	-4.33	-1.09
NZP10	outcrop	3.85	4.56	-6.18	-5.38
Eddystone 5	1256.2	-3.70	3.50	-11.90	-5.20
Eddystone 5	1219.3	4.02	4.40	-4.50	-2.26

Outcrop samples were analysed to help complete sequences if suitable drill core material was unavailable when the biostratigraphical control on the outcrop samples was good. Palynology and lithostratigraphy indicated the stratigraphical order of samples from different coreholes with respect to one another and identifed sampling gaps.

4.3 Results and discussion

$\delta^{13}C_{CO3}$, $\delta^{13}C_{org}$, and $\delta^{18}O_{CO3}$ values are listed in Table 4.2. Δ ($\delta^{13}C_{CO3}$ - $\delta^{13}C_{org}$) is constant under fixed CO_2 pressures (Hayes et al., 1989; Magaritz et al., 1992) and was in the range -27 to -31‰ for most sample pairs. The lower limit of Δ from Eastern Australia (Table 4.2) is similar to values determined on sediments in the Gartnerkofel Core-1 section in Austria (Magaritz et al., 1992, table 1) where the average Δ of samples from the Late Permian Bellerophon Formation is -26.84‰ (17 determinations) and from the Early Triassic Werfen Formation -27.29‰ (15 determinations). Magaritz et al. (1992) suggest that little weight be given to sample pairs where the Δ exceeds 30‰ because of the likelihood of the samples having undergone alteration. Knoll et al. (1986) suggest that Δ values within the range 28.5‰ ±2‰ indicate a high probability of primary values having been preserved within a few ‰. Some of the sample pairs from the Bowen Basin sections have Δ values up to 32.5‰, larger than 30‰ but the fabric retentive, non-luminescent character of the brachiopod shells suggest preservation of a primary isotope signature (Popp et al., 1986a; Hudson and Anderson, 1989; Bates and Brand, 1991) and the general trend is for the $\delta^{13}C_{org}$ in the sample pairs to be more negative than samples stratigraphically adjacent. More negative $\delta^{13}C_{org}$ suggests a primary signature as organic matter commonly becomes more positive with biodegradation or alteration as the lighter carbon isotope is more likely to be involved in chemical reactions and lost as a volatile (Hayes et al., 1989). Despite reservations about rejecting sample pairs with Δ >30‰, values outside the range -27 to -31‰ are treated here as suspect. Other possibilities such as:

1) The $\delta^{13}C_{org}$ sample may be representative of a peculiar microenvironment that resulted in the addition of methanotrophic biomass with a very negative $\delta^{13}C_{org}$, or

2) Preferential preservation of compounds that tend to be enriched in the lighter isotope of carbon such as lipids has occured (Hayes et al., 1989), lie beyond the scope of this study.

Table 4.2 Carbonate carbon isotope results.

Location	depth m	$\delta^{13}C_{CO3}$‰	$\delta^{18}O_{CO3}$‰	$\delta^{13}C_{org}$‰	TOC%	Δ‰	C.L.	Palynology	Shell	Formation
GSQ E-1	647	5.00	-0.43	-25.26	0.5	30.26	nlum	U5	Sp	Peawaddy
GSQ E-1	692	4.16	-2.81	-23.57	1.4	27.77	nlum	U5	P	Ingelara
GSQ E-1	701.8	6.40	-0.30	-23.40	1.8	29.80	nlum	U5	Sp	Ingelara
GSQ E-1	702	6.83	0.03	-23.22	2.0	30.02	nlum	U5	Sp	Ingelara
GSQ E-1	784	5.82	-0.98	-23.91	3.2	29.71	nlum	U5	P	undiff
GSQ E-1	793.1	4.25	-3.31				nlum	L5c	Sp	undiff
GSQ E-1	937	7.83	-1.33	-24.18	1.8	31.98	nlum	U4a	Sp	undiff
GSQ E-1	947	6.76	-1.56	-23.02	1.3	29.82	nlum	U 4a	Sp	undiff
GSQ E-1	973.5	5.34	0.05				nlum	L 4/3b	Sp	Reids Dome
GSQE-5	735	2.36	-3.24	-24.61	2.1	26.97	nlum	U5	P	Peawaddy
GSQE-5	833	5.03	-2.03	-23.47	0.3	28.50	nlum	U5	Sp	Freitag
GSQE-5	861.3	7.30	-2.80				nlum	UL5	Sp	Aldebran
GSQE-5	864.35	4.40	-2.34	-25.65	0.3	30.04	nlum	UL5	Sp	Aldebran
GSQE-5	864.35	4.34	-1.24				nlum	UL5	Sp	Aldebran
GSQE-5	972.59	4.60	-2.54				nlum	U 4b-UL5	P	Aldebran
GSQE-5	1196.84	7.55	-0.94	-23.67	0.8	31.27	nlum	U4a	Sp	Cattle Ck
GSQE-5	1210.6	6.52	-0.73	-23.89	2.4	30.41	nlum	U 4a	Sp	Cattle Ck
GSQE-5	1210.6	5.08	-0.53				nlum	U4a	Sp	Cattle Ck
GSQE-5	1219.3	4.38	-2.51				nlum	U4a	St	Cattle Ck
GSQE-5	1219.3	4.40	-2.26	-23.16	1.2	27.56	nlum	U 4a	St	Cattle Ck
GSQE-5	1219.3	4.02	-4.49	-23.16	1.2	27.17	**plum**	U 4a	P	Cattle Ck
GSQE-5	1256.2	3.50	-5.20	-23.80	1.1	27.30	**plum**	U4a	P	Cattle Ck
GSQE-5	1302.2	6.07	-1.55	-22.89	1.1	28.99	nlum	U4a	Sp	Cattle Ck
GSQE-5	1306	5.34	-3.64	-27.13	1.9	32.43	nlum	U 4a	Sp	Cattle Ck
GSQE-5	1316.2	5.50	-2.65				nlum	U4a	P	Cattle Ck
GSQ S-19	514.6	5.25	-2.68				nlum	U5	P	Mantuan
GSQ S-19	516.68	5.38	-2.27				nlum	U5	P	Mantuan
GSQT-10	831.25	2.46	-4.12				**plum**	U4b	P	Cattle Ck
GSQT-10	831.25	3.50	-3.45	-23.30	2.5	26.80	nlum	U4b	P	Cattle Ck
GSQT-10	838.2	4.22	-1.28	-23.98	2.0	28.18	nlum	U4b	P	Cattle Ck
GSQT-10	844.28	5.64	-3.03	-23.87	2.8	29.51	nlum	U4b	P	Cattle Ck
GSQT-10	845.25	4.66	4.85				**plum**	U4b	P	Cattle Ck
GSQT-10	845.25	4.29	-2.82	-23.99	2.7	28.29	nlum	U 4b	P	Cattle Ck
GSQT-10	845.25	4.46	-3.09	-23.99	2.7	28.39	nlum	U4b	P	Cattle Ck
GSQT-10	861.3	7.35	-2.84	-25.08	2.6	32.42	nlum	U4b	Sp	Cattle Ck
GSQT-10	864.35	4.34	-1.24				nlum	U4b	Sp	Cattle Ck
GSQT-10	864.7	4.24	-4.33				**plum**	U4b?	P	Cattle Ck
GSQT-10	868.8	5.29	-2.41	-23.77	0.9	29.07	nlum	U4a	P	Cattle Ck
GSQT-10	872.6	6.73	-2.55	-23.97	1.4	30.71	nlum	U4a	P	Cattle Ck

Table 4.2 continued.

Location	depth m	$\delta^{13}C_{CO3}$ ‰	$\delta^{18}O_{CO3}$ ‰	$\delta^{13}C_{org}$	TOC%	Δ‰	C.L.	Palynology	Shell	Formation
GSQT-10	884.4	6.90	0.30				nlum	U4a	Sp	Cattle Ck
GSQT-10	890.7	5.50	-1.98	-23.37	2.70	28.87	**plum**	U4a	Sp	Cattle Ck
GSQT-10	897.2	6.96	-1.19				nlum	U4a	Sp	Cattle Ck
GSQT-10	897.2	7.78	-0.87				nlum	U4a	Sp	Cattle Ck
GSQT-10	897.2	6.92	-0.04				nlum	U4a	Sp	Cattle Ck
GSQT-10	909.75	6.54	-1.37				nlum	U4a	Sp	Cattle Ck
GSQT-10	926.8	5.62	-0.76	-25.05	0.60	30.67	nlum	U4a	Sp	Cattle Ck
GSQT-10	926.8	5.75	-1.22				nlum	U4a	Sp	Cattle Ck
GSQT-10	939.9	6.84	-2.03				nlum	U4a	Sp	Cattle Ck
GSQT-10	946.45	7.46	-1.09	-22.97	2.30	30.43	nlum	U4a	Sp	Cattle Ck
GSQT-10	952.39	6.89	-1.38	-23.31	1.80	30.21	nlum	U4a	Sp	Cattle Ck
GSQT-10	959.9	6.33	-0.96	-23.00	2.70	29.34	nlum	U4a	Sp	Cattle Ck
GSQT-10	959.9	6.34	-0.38				nlum	U4a	Sp	Cattle Ck
HB11-1		5.70	0.10				nlum	U5	Sp	Cherrabun M
HB11-2		2.80	-1.40				**plum**	U5	Sp	Cherrabun M
NZD45/f7574		1.94	-4.13				nlum	Smithian?	Sp	Malakoff Hill
NZH46/f146		3.12	-5.32				nlum	Carnian?	T	unnamed
NZF7/f6540		2.28	-5.68				**plum**	latest Permian?	Ch	Titiroa L'stone
NZC2		-0.19	-2.77				nlum	Ladinian	Sp	Clinton Fm
NZP10		4.56	-5.38				**plum**	latest Permian?	B	Wairaki b
NZP10		3.85	-6.18				Lum	latest Permian?	B	Wairaki b
UQ 4643		5.26	-1.52				nlum	L5c	P	
UQL3543		5.15	-3.26				nlum	uL5c	P	Scottsville M.
UQ 5129		4.70	-0.51				nlum	U 4b	P	Fenestella Sh.
UQ 5124		5.46	-1.46				**plum**	U4b	P	Elderslie Fm
UQ 5124		6.17	-1.63				nlum	U4b	P	Elderslie Fm
UQL2421		4.78	-0.58				nlum	U5	P	Peawaddy

Sp = Spiriferid; P = Productid; St = Strophomenid; Ch = Chonetid; B = Bivalve; T = Terebratulid; plum = part luminescent; lum = fully luminescent; nlum = nonluminescent.

In Eddystone-1 (Fig.4.1) a $\delta^{13}C_{CO3}$ and $\delta^{18}O_{CO3}$ study was made using calcite from nonluminescent brachiopods. $\delta^{13}C_{CO3}$ values between 4 to 7.8‰, generally heavier than typical whole-rock carbonate values on the Tethyan margin (Baud et al., 1989) and South China (Chen et al., 1991; Xu and Yan, 1993), are similar to Late Permian brachiopod calcite $\delta^{13}C_{CO3}$ values from Sichuan China (Gruszczyñski et al., 1990) and to *Neospirifer* brachiopod calcite samples from the Hardman Formation, Canning Basin (Compston, 1960). The $\delta^{18}O_{CO3}$ values of brachiopods from GSQ Eddystone-1 are similar to those determined on *Neospirifer* from the Hardman Formation but are more positive than those of Late Permian brachiopods from Sichuan (Gruszczyñski et al., 1990) or from whole-rock $\delta^{18}O_{CO3}$ sections on Tethys and South China marine margins (Baud et al.,1989; Chen et al., 1991).

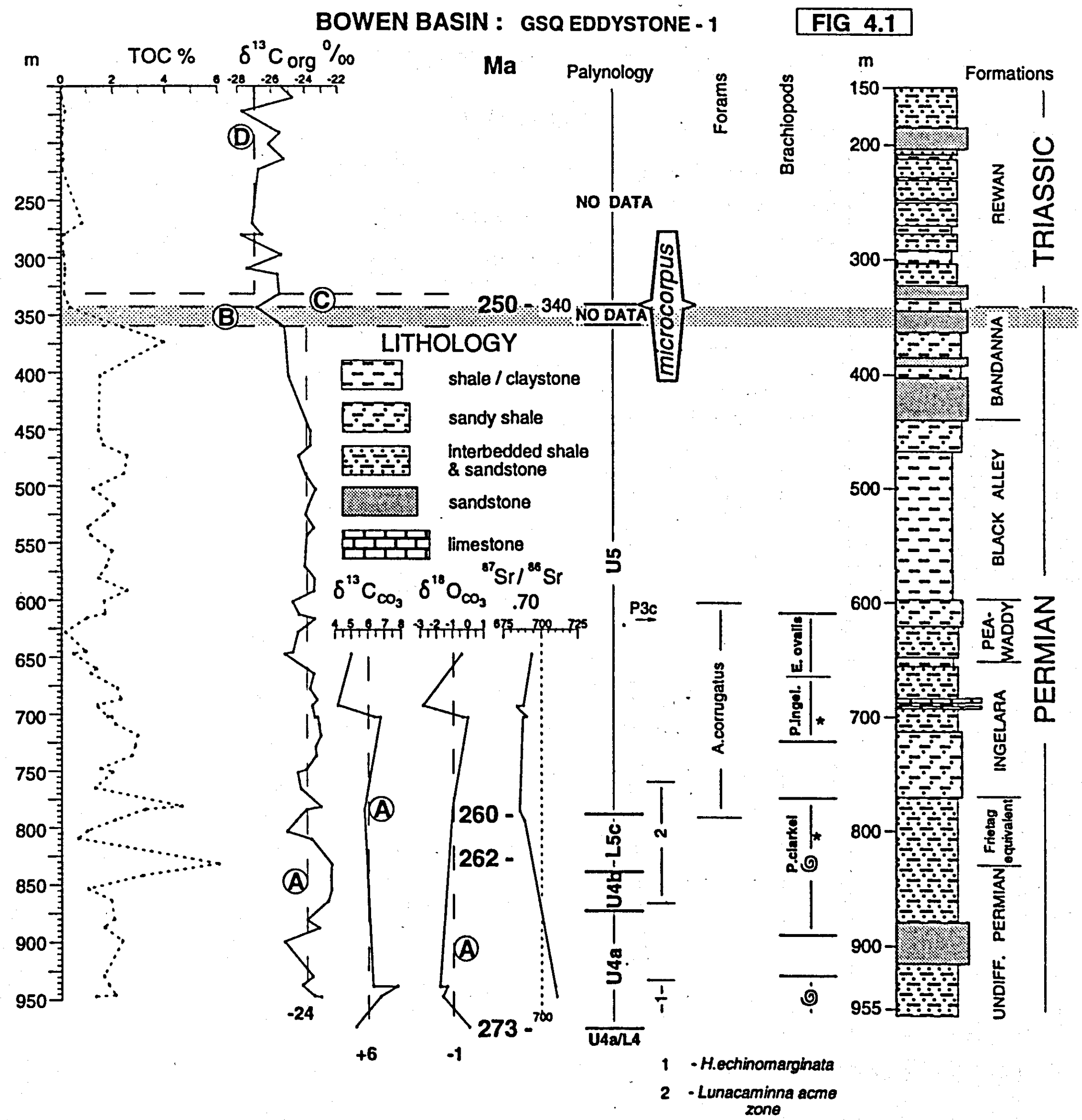

Figure. 4.1 Eddystone-1, Bowen Basin, eastern Australia. Total organic carbon (TOC), $\delta^{13}C_{org}$, $\delta^{13}C_{CO3}$, $\delta^{18}O_{CO3}$, $^{87}Sr/^{86}Sr$, palynological zones (McKellar, 1978), foraminifera zones (Palmieri,1983), brachiopod zones (D. Briggs pers. comm., 1992), lithological log, and formations (Heywood, 1978). Determinations on carbonate samples are from non-cathodoluminescent brachiopods. The negative $\delta^{13}C_{org}$ excursion is between values of -24‰ for the Permian and -27‰ for the Triassic. The line at 340 m is my pick of the Permian-Triassic boundary, and it coincides with the base of the Rewan Formation and the first determined sample of the Tr1a (= *P. microcorpus*) zone (McKellar, 1978).

In Eddystone-5 (Fig.4.2), $^{13}C_{CO3}$ values from nonluminescent brachiopod calcite are within the range 4 to 8‰ with a single exception, a low of 2.35‰ in the topmost Ingelara Formation at 735 m. There is no clear pattern of secular variation in the $\delta^{13}C_{CO3}$ determinations in this corehole although there is slight trend towards more negative $\delta^{13}C_{CO3}$ up sequence. The $\delta^{13}C_{CO3}$ of non-luminescent brachiopod calcite ranges about a central value of 6‰, displaced approximately 30‰ from $\delta^{13}C_{org}$ average of about -24‰. Upper Stage 4 $\delta^{13}C_{CO3}$ values range from 4.4 to 7.6‰, Lower Stage 5 from 4.4 to 7.3‰ and in Upper Stage 5 between 5.1 and 2.34‰. The $\delta^{18}O_{CO3}$ values from non-luminescent brachiopod shells in Upper Stage 4 range from -0.5 to -3.6‰, within upper Lower Stage 5 are between -1.2 and -2.8‰, and in Upper Stage 5 are between - 2 and - 3.3‰.

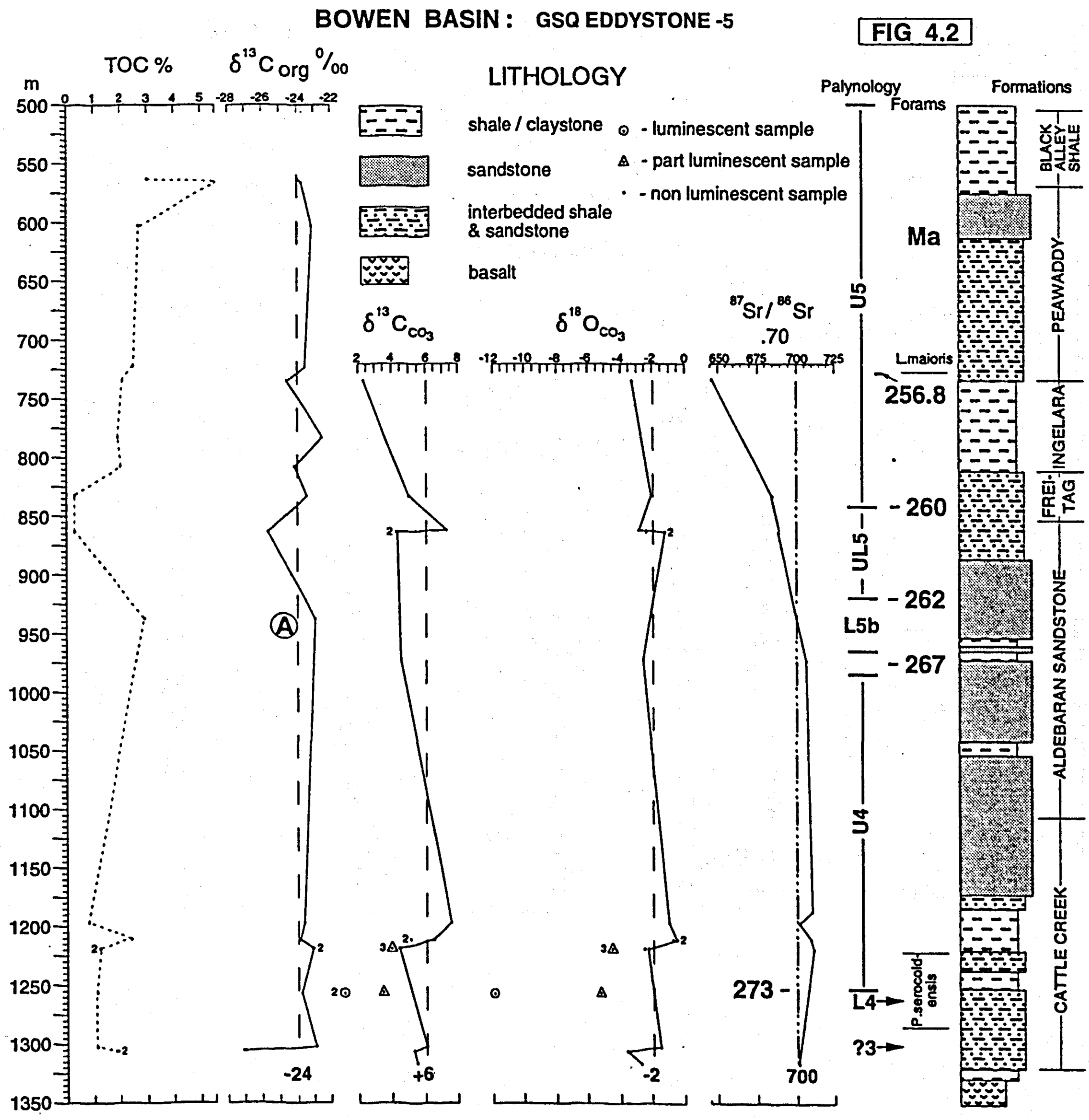

Figure 4.2 Eddystone-5, Bowen Basin, eastern Australia. Total organic carbon (TOC), $\delta^{13}C_{org}$, $\delta^{13}C_{CO3}$, $\delta^{18}O_{CO3}$, $^{87}Sr/^{86}Sr_{CO3}$, palynological zones (Jones, 1986), foraminifera zones (Palmieri,1983), brachiopod zones (Briggs pers. comm., 1992), lithological log, and formations (Draper & Green, 1983). Determinations on carbonate samples are from non-luminescent (nlum) brachiopods, except at 1219.3 m which was a partly luminescent (plum) specimen.

In Taroom-10 (Fig.4.3) a study of $\delta^{13}C_{CO3}$ and $\delta^{18}O_{CO3}$ was confined to Upper Stage 4 sediments of the Cattle Creek Formation. Over the interval of the study the $\delta^{13}C_{CO3}$ of non-luminescent brachiopod calcite ranges from 3.5 to 7.8‰ about a central value of 6‰, displaced approximately 30‰ from $\delta^{13}C_{org}$ of -24‰, as in Eddystone-5. The $\delta^{18}O_{CO3}$ ranges between 0.3 and -4.2‰.

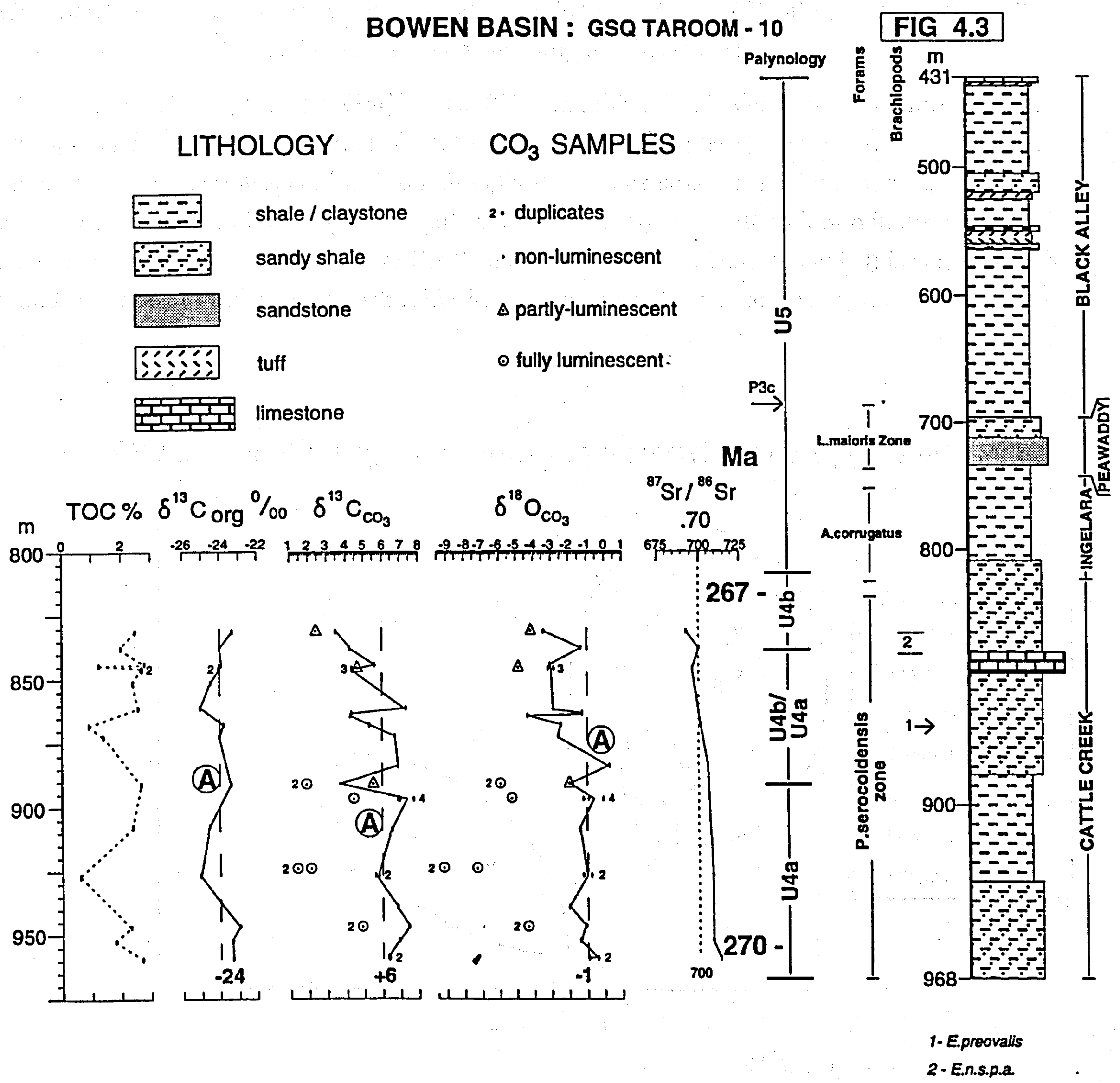

Figure 4.3 Taroom-10, Bowen Basin, eastern Australia. Total organic carbon (TOC), $\delta^{13}C_{org}$, $\delta^{13}C_{CO3}$, $\delta^{18}O_{CO3}$ (relative to PDB), $^{87}Sr/^{86}Sr_{CO3}$, palynological zones (McKellar, 1978), foraminifera zones (Palmieri,1983), brachiopod zones (Briggs pers. comm., 1992), lithological log and formations (Draper & Green, 1983).

Fig. 4.4 shows a plot of $\delta^{18}O_{CO3}$ versus $\delta^{13}C_{CO3}$ of the total non-luminescent brachiopod data set. Almost the entire dataset of $\delta^{13}C_{CO3}$ from Permian Australian and New Zealand brachiopods examined in this study are > 4‰. This is similar to the $\delta^{13}C_{CO3}$ results on Permian brachiopods from the Canning Basin (Compston, 1960) and Tasmania (Rao and Green, 1982; Rao, 1988). The data from the Triassic are New Zealand shelly faunas and, having more negative $\delta^{13}C_{CO3}$ and $\delta^{18}O_{CO3}$ values do not plot in the same field as samples from the Australian Permian sequences. The samples labelled "x" and "y" are atypical Australian Permian samples and may represent undetected alteration or a peculiar environment of deposition that affected the isotopic values. Both "x" and "y" have low $\delta^{18}O_{CO3}$ and this may indicate some undetected diagenetic alteration. Interestingly sample "x" (GSQE-5 735 m) also has an atypical extremely low $^{87}Sr/^{86}Sr$ ratio (Table 3.2), which might indicate a peculiar alteration.

The three samples from GSQT-10 at 897.2 m (Table 4.2) indicate the variability of $\delta^{13}C_{CO3}$ and $\delta^{18}O_{CO3}$ in samples from the same stratigraphic level. These samples were taken from different nonluminescent brachiopod shells at the same stratigraphic level and suggest that any data obtained from brachiopods is quite variable and might be better viewed in the context of an average from a number of shells rather than individual results. Unfortunately this was generally beyond the scope of this study which relies heavily upon single carbonate analyses for a particular stratigraphic level.

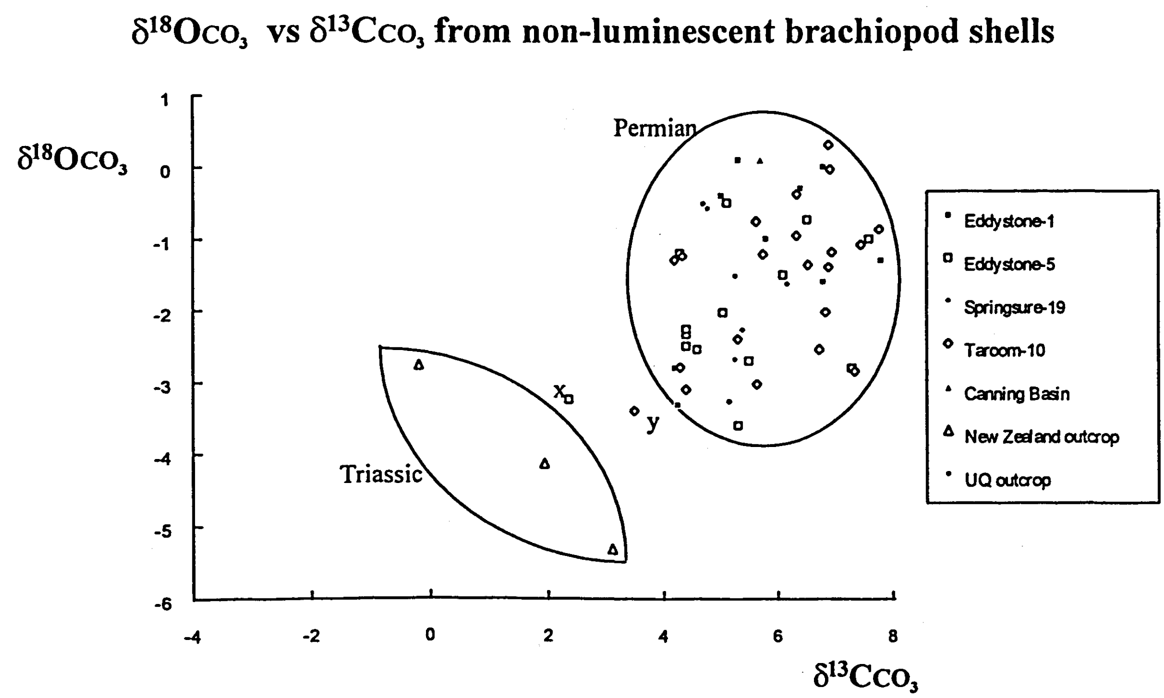

Fig. 4.4 $\delta^{18}O_{CO3}$ vs $\delta^{13}C_{CO3}$ for non-luminescent Permian and Triassic brachiopod shells.

Plotting $\delta^{18}O_{CO3}$ vs Δ (Fig. 4.5) appears to suggest some correlation. This indicates either 1) a decrease in Δ as the $\delta^{18}O_{CO3}$ decreased and presumably temperature of seawater increased. This could have resulted from a lower pressure of CO_2 in warmer surface waters due to decreased solubility resulting in an increase in the $\delta^{13}C_{org}$ of marine organic matter while the $\delta^{13}C_{CO3}$ remained largely unaffected, or 2) it may also reflect undetected alteration as $\delta^{18}O_{CO3}$ usually becomes more negative with increasing alteration while Δ tends to become smaller. The screening of the samples does not support this option, however, and suggests the trend towards lower Δ values in the Upper Stage 5 Zone is a result of higher seawater temperatures.

4.4 Conclusions

The average value of Δ ($\delta^{13}C_{CO3}$-$\delta^{13}C_{org}$) of the Bowen Basin sample pairs analysed is -29.43‰ (30 pairs) (Table 4.2). Δ decreases between the Early Permian (average 29.52‰) and the early Late Permian (average 29.13‰). All Δ values greater than 30.5‰ (n = 6) are from sample pairs interpreted as Artinskian and Kungurian when there is evidence of ice rafted material in fine grained marine sediments (Draper, 1983).

Δ values from the Gartnerkofel Core-1, Southern Carnic Alps about the Permian-Triassic boundary are younger (Changxingian/Griesbachian) than those of the Bowen Basin and average about 27‰ (Magaritz et al., 1992), lower than those of both the Early and early Late Permian of the Bowen Basin. This could reflect a warmer low latitude environment of deposition where decreased solubility of CO_2 results in more positive $\delta^{13}C_{org}$ values (Rau et al., 1989) or could reflect a global trend toward smaller Δ values through the Late Permian and Early Triassic.

The later proposition implies a lower atmospheric CO_2 pressure and hence a cooler climate (Magaritz et al., 1992). The reverse of this appears true with no evidence of ice in the Latest Permian even in Eastern Australia (Dickins, 1993, fig. 1) which was at that time close to the pole (Lackie and Schmidt, 1993).

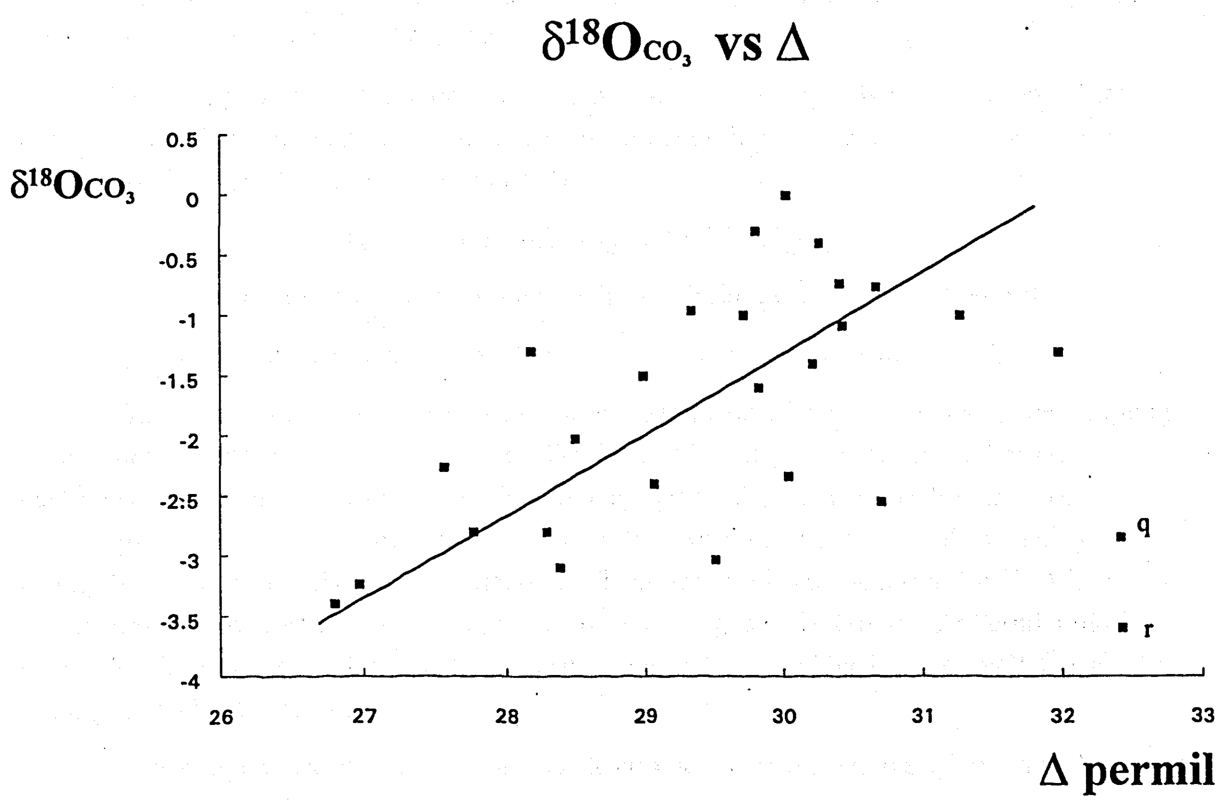

Fig. 4.5. $\delta^{18}O_{CO3}$ vs Δ for non-luminescent brachiopods from the Bowen Basin.

4.5 Paleotemperature estimates from the Permian Panthalassan margin sediments of Eastern Australia

$\delta^{18}O_{CO3}$ values from unaltered low magnesium calcite brachiopod shells that have grown in equilibium with seawater can be used as paleothermometers (Urey et al., 1948; McCrea, 1950; Hudson and Anderson, 1989; Marshall, 1992). The determination of $\delta^{18}O_{CO3}$ and $\delta^{13}C_{CO3}$ of non-luminescent brachiopods in the Denison Trough region of the Bowen Basin enables an paleotemperature record of this region to be estimated during Lower Stage 4 to Upper Stage 5.

Rao and Green (1982) and Rao (1988) estimated paleotemperatures of the Permian seas on the Eastern Australian Panthalassan margin from Stage 3a to Lower Stage 4 using brachiopods from Tasmanian sedimentary basins. Spiriferid brachiopod samples from the Darlington Limestone (Rao and Green, 1982, table 1) of palynological zone Stage 3a (Clarke et al., 1989; fig. 8.1) have $\delta^{18}O_{CO3}$ in the range -4.4 to -0.7‰ and $\delta^{13}C_{CO3}$ in range 4.7 to 6.3‰ respectively. These thick shelled *Spiriferids,* not evaluated for diagenetic alteration using a cathodoluminescent microscope, probably provide an accurate record of $\delta^{13}C_{CO3}$ and $\delta^{18}O_{CO3}$ (Grossman, 1994, p. 217) because shells with thick prismatic layers are resistant to diagenesis. Brachiopods (unidentified family) from the Berriedale Limestone (Rao, 1988, table 1) of palynological zone Stage 4 (Clarke et al., 1989, fig 8.1) have $\delta^{18}O_{CO3}$ and $\delta^{13}C_{CO3}$ in the ranges -6.4 to -0.9‰ and 3.4 to 5.4‰ respectively. The possibility of diagenetic alteration of these samples from the Berriedale Limestone cannot be discounted but the $\delta^{13}C_{CO3}$ values are similar to values from Stage 4 samples from the Denison Trough (Table 4.2) that were screened for alteration. This indicates "heavy" $\delta^{13}C_{CO3}$ values persist from at least Stage 3a (Asselian) to within Upper Stage 5 in brachiopods from Eastern Australia.

Paleotemperature is estimated for Bowen Basin samples by palynological zone (Table 4.3) using the Shackleton and Kennett (1975) equation developed for cold water sediments similarly to the procedure used by Rao (1988).

$$T(°C) = 16.9 - 4.38\ (\delta_c - \delta_w) + 0.10\ (\delta_c - \delta_w)^2$$

where δ_w = the isotope composition of the CO_2 in equilibrium with the formation water.

δ_c = the isotope composition of CO_2 produced from the carbonate at 25°C.

This equation is appropriate for use throughout the time interval covered by the sampling in this study because the last dropstones (indicating a cold water environment) in Eastern Australia are from the Dempsey Formation, Sydney Basin (Veevers et al, 1994) that is of palynological zone Upper Stage 5 and because Eastern Australia was close to the magnetic (? = geographic pole) during the Late Permian/Early Triassic (Lackie and Schmidt, 1993). A high latitude position of Australia is also supported by paleomagnetic data from Late Permian/Early Triassic sediments with high magnetic inclination angles from the Merrimelia-3 well, Cooper Basin (Fig 2.33; Chapter 5).

Paleotemperature estimates have been determined for palynostratigraphic intervals using the following assumptions:

1) δ_w is assumed to have been a constant -2.8 ‰, a value determined by Given and Lohman (1986) for the Permian. This value in all likelihood changed as ice-caps waned during the Permian

however estimating a variation in δ_W through the Permian and still retaining the validity of sample comparison would involve circular argument so it is preferred to use a fixed δ_W = -2.8‰.

2) The paleotemperature range estimate for any palynological zone is determined from the extreme $\delta^{18}O_{CO3}$ values from noncathodoluminescent brachiopod shells. The average paleotemperature for a palynological zone is determined from the mean $\delta^{18}O_{CO3}$ value of the brachiopod shells of each palynology zone. By using a mean value of $\delta^{18}O_{CO3}$ for determining temperature there may be the advantage of obtaining an average temperature rather than a seasonal temperature or one determined by conditions of the local habitat of a single shell.

3) The brachiopods are assumed to have not fractionated oxygen as a result of vital effects, phylogenetic or habitat differences.

4) Palynology zones are assumed isochronous across regions. No distinction is made on the basis of relative position within a palynology zone.

5) Only samples from the Denison Trough found in coreholes have been used to estimate paleotemperature. These samples are from a limited geographical area and because they come from core are less likely to have been diagenetically altered during weathering.

All of these assumptions are questionable, however, an average of $\delta^{18}O_{CO3}$ values derived from brachiopods across each palynology zone interval does provide an indication of relative paleotemperature and environmental variations.

4.6 Results

The paleotemperature analysis by palynological zone in the Bowen Basin is shown in Table 4.3.

Table 4.3 Oxygen isotope values and estimated temperatures.

Palynology zone	$\delta^{18}O_{CO3}$ range‰	T°C range	$\delta^{18}O_{CO3}$ average‰	T°C average
Upper Stage 5	-3.2 to 0	18.8 to 4.4	-1.6	11.9
u Lower Stage 5	-3.3 to -1.2	19.1 to 10.1	-2.4	15.2
Upper Stage 4b	-3.4 to -1.24	19.6 to 10.3	-2.5	15.7
Upper Stage 4a	-3.6 to 0.3	20.5 to 3.7	- 1.4	11

Average data based upon 9 analyses Upper Stage 5, 4 analyses u Lower Stage 5, 8 analyses Upper Stage 4b, and 24 analyses Upper Stage 4a.

4.7 Conclusions

Paleotemperatures calculated using $\delta^{18}O_{CO3}$ for unaltered brachiopods from the Bowen Basin analyses indicate water temperatures which are unrealistic for the inferred high polar latitude of the Denison Trough at the time of deposition. An explanation for the anomalously high paleotemperature estimates is that the shelf seawater was diluted with melt water from icesheets, sea ice or meteoric water. Rao (1988) suggests a similar scenario for the brachiopod shell material from the Berriedale Limestone of Tasmania. The presence of erratic dropstones and pebbles in sediments throughout the greater part of the Denison Trough sequence from the Reids Dome Beds through to the Peawaddy Formation is evidence of ice on the sea surface and supports this explanation (Draper, 1983). The origin of the ice is unclear but is hypothesised to be from a source feeding into the Denison Trough and river ice is suggested by Draper (1983). $\delta^{18}O_{CO3}$ values of melt water, possibly in the range of -60‰ PDB, would have significantly reduced the $\delta^{18}O_{CO3}$ values of carbonate forming in the marine shelf environment where brachiopods inhabited.

The higher estimated paleotemperatures for Upper Stage 4b and upper Lower Stage 5 (Table 4.3) are based upon small data sets (4 and 8 samples respectively) but is similar for these two sequential palynology zones. The paleotemperature estimate of around 15-16° C for stages Upper Stage 4b and uLower Stage 5 is higher than that for Upper Stage 4a or Upper Stage 5 (Table 4.3). This could be interpreted to reflect an increased level of freshwater runoff to the marine shelf during this period compared to either Upper Stage 4a or Upper Stage 5 and is supported by the Upper Stage 5 estimated temperature being lower than that for uLower Stage 5 to Upper Stage 4b even though the lithostratigraphical evidence of ice appears to have declined by Upper Stage 5.

A weak correlation exists between Δ and $\delta^{18}O_{CO3}$ (Fig 4.5). This shows that as $\delta^{18}O_{CO3}$ decreases Δ also tends to decrease. The samples "q" and "r" (Fig 4.5) have very negative $\delta^{13}C_{org}$ values compared to samples adjacent in their respective sections as well as having relatively negative $\delta^{18}O_{CO3}$ and therefore may represent undetected diagenetic alteration.

APPENDIX 4.1

Location of outcrop samples analysed for carbon and oxygen stable isotopes.

Table 4.4 Locality of outcrop samples.

Sample locality No.	**BASIN**	**SUB-BASIN**	**Locality Description; formation.**
NZD45/f7574	Southland Geosyncline		Grid ref. 184663 North side Coal Ck; Malakoff Hill Group.
NZH46/f146	Southland Geosyncline		Grid ref. 634154 Hays Gap, Nugget Point coast; unnamed.
NZF7/f6540	Southland Geosyncline		Grid ref. 8587 0887 Titaroa Stream; Titaroa Limestone
NZC2	Southland Geosyncline		Lat. 46°12' 48", Long. 169°21' 45" Kuriwao Gorge Rd; Murihiku Limestone
NZP10	Southland Geosyncline		Lat. 45°46'45", Long. 167°58' 6" Wairaki Breccia
NZP10	Southland Geosyncline		Lat. 45°46'45", Long. 167°58' 6" Wairaki Breccia
HB11	Canning	Fitzroy Trough	Lat. 19°5' 36", Long. 125°9' 45" Cherruban Mbr, Mt Hardman.
UQ L2421	Bowen	Denison Trough	Mantuan Horizon, Peawaddy Fm, Reids Dome Rd, 3.25 km from the Rewan-Rolleston Rd.
UQ L3543;	Bowen	Denison Trough	Lat. 20°50' approx.; Long. 147°42' approx. Scottsville Mbr., Blenheim Fm.
UQ 5124 = NE L1229	Sydney		Hunter Valley, western end of road cut on Kurri Kurri- Mulbring Rd, Elderslie Fm.
UQ 5129	Sydney		Hunter Valley, east end of railway cut west of road overpass at Branxton, Fenestella Shale.

UQ = University of Queensland fossil locality. NE = University of New England fossil locality.

5. PALEOMAGNETIC STRATIGRAPHY ABOUT THE PERMIAN-TRIASSIC BOUNDARY IN AUSTRALIA

5.1 Paleomagnetism in the Merrimelia-3 borehole, Cooper Basin

Of the extant boreholes in the Cooper Basin Merrimelia-3 is unique in that it is almost fully cored about the Permian-Triassic boundary making it ideal for a $\delta^{13}C_{org}$ and paleomagnetic stratigraphy study. The negative $\delta^{13}C_{org}$ excursion about the Permian-Triassic boundary in the Merrimelia-3 borehole (see Fig. 2.32 for location) has been discussed in Chapter 2. The paleomagnetic stratigraphy is discussed below.

Cooper Basin sediments straddling the Permian-Triassic boundary were deposited at approximately 80° S (Lackie and Schmidt, 1993) and appear to have retained their original magnetic polarities without the overprint found in eastern Australia. Accordingly, because of the high paleolatitude, the polarity of the core (reversed or normal) can be determined without the need to orient the core as would be necessary with sediments deposited at lower paleolatitudes.

The Permian-Triassic sedimentary sequence in the intracontinental Cooper Basin was probably more fully recorded than in the foreland sedimentary basins of eastern Australia (Veevers, Conaghan and Powell, 1994) that were prone to regressional erosion during the sealevel fall about the Permian-Triassic boundary (Holser and Magaritz, 1987; Ross and Ross, 1987). These sediments are ideal for a study of paleomagnetic stratigraphy about the Permian-Triassic boundary.

5.2 Methods

A magnetostratigraphical study of 40 samples from Merrimelia-3 established that only fine sandstones have stable natural remanent magnetisation (NRM) and that many of these have reversed polarity. Remanences were measured using a 3-axes CTF 200 model cryogenic magnetometer interfaced to a PC for automatic measurement control and data handling. Samples were subjected to step-wise demagnetisation with a Schonstedt GSD-1 instrument (AF) or an in-house zero-field furnace (thermal demagnetisation). Because thermal demagnetisation of the samples often causes large increases in magnetic susceptibility above 300°C and erratic changes of remanence, alternating field (AF) demagnetisation was mostly used after all samples were first heated to 180°C to eliminate goethite.

Straight-line segments were fitted to the demagnetisation trends using in-house software to perform principle component analysis. Subsequently, the remanance inclinations were plotted against stratigraphic level to aid identification of different polarity intervals.

5.3 Results

The cleaned data from samples about the Permian-Triassic boundary are shown in Fig. 5.1 and are listed in Table 5.1. Figure 5.2 shows the intensity, stereographic and orthogonal plots of thermal or AF demagnetisation of selected representative specimens from normal and reversed intervals about the negative $\delta^{13}C_{org}$ excursion at 2362 m taken to indicate the Permian-Triassic boundary.

The fine-sandstone samples typically exhibit uni-vectorial components and NRM intensities of between 1 to 2 mAm^{-1} with median destructive fields (MDFs) of 20-30 mT. Dark siltstones and mudstones are unstably magnetised, and after AF or thermal demagnetisation the remanence vectors are erratic so these samples are not considered in this analysis.

In the stratigraphic section below the $\delta^{13}C_{org}$ excursion at 2362 m all samples with a well-defined magnetic polarity have a reversed polarity. The $\delta^{13}C_{org}$ excursion about the Permian-Triassic boundary lies 4 m above the last reversed sample at 2366 m and between samples from the *Weylandites* and *P. microcorpus* Zones.

Table 5.1. Merrimelia-3 magnetic inclination.

Corehole	Depth m	Inclination °
Merrimelia-3	2252	64
Merrimelia-3	2286	82
Merrimelia-3	2289	78
Merrimelia-3	2292	70
Merrimelia-3	2294.4	74
Merrimelia-3	2294.4	78
Merrimelia-3	2300	-72
Merrimelia-3	2301.2	-69
Merrimelia-3	2308.2	84
Merrimelia-3	2309	79
Merrimelia-3	2309.1	85
Merrimelia-3	2315.4	77
Merrimelia-3	2318	79
Merrimelia-3	2325	84
Merrimelia-3	2326	85
Merrimelia-3	2326	87
Merrimelia-3	2348	-80
Merrimelia-3	2349.6	-58
Merrimelia-3	2366.92	68
Merrimelia-3	2369.6	81
Merrimelia-3	2387.71	52
Merrimelia-3	2394	75
Merrimelia-3	2403.5	67
Merrimelia-3	2405.7	77
Merrimelia-3	2405.7	74
Merrimelia-3	2408.5	73
Merrimelia-3	2408.6	76
Merrimelia-3	2409.45	78
Merrimelia-3	2409.45	76
Merrimelia-3	2412.8	78

Note: positive values of inclination are reversed, negative values are normal polarity. No bedding corrections have been applied because the dip was usually much less than 10° and hence would have limited effect on the inclination values, and additionally the core was not oriented azimathally.

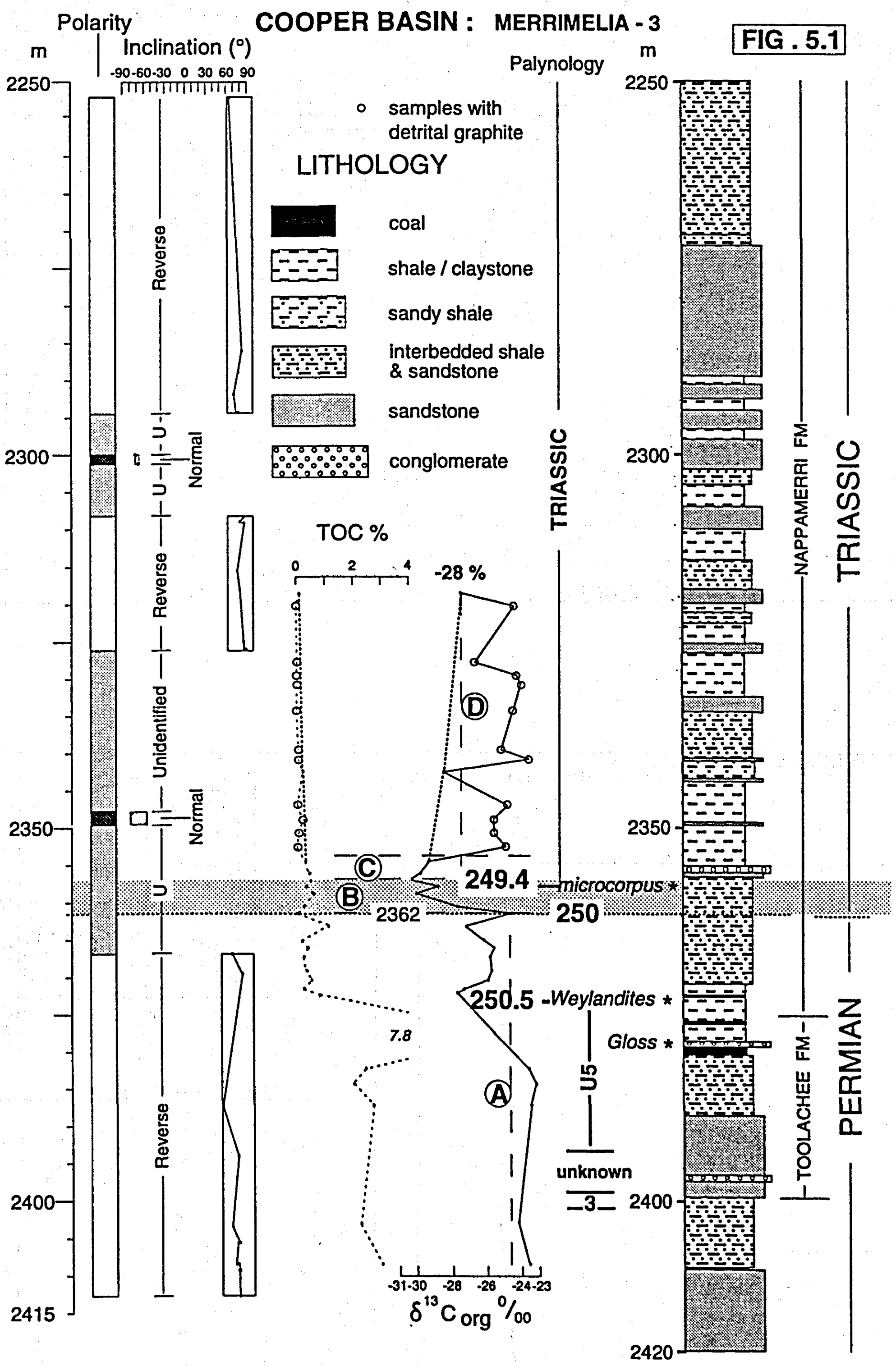

Figure 5.1 Merrimelia-3, Cooper Basin, central Australia. Magnetic polarity, total organic carbon (TOC), $\delta^{13}C_{org}$, palynological zones from G. Woods pers. comm. (1993), Paten, (1966), Kemp et al.(1977, p. 191), lithological log and formations (Delhi Australia Petroleum Ltd, 1965). The negative $\delta^{13}C_{org}$ excursion between mean values of –24.8 ‰ and -30 ‰ lies between samples from the *Weylandites* Zone at 2373.17 m (Kemp et al. 1977, p. 191) and the *P. microcorpus* Zone at 2357.93 m (G. Woods pers. comm. 1993).

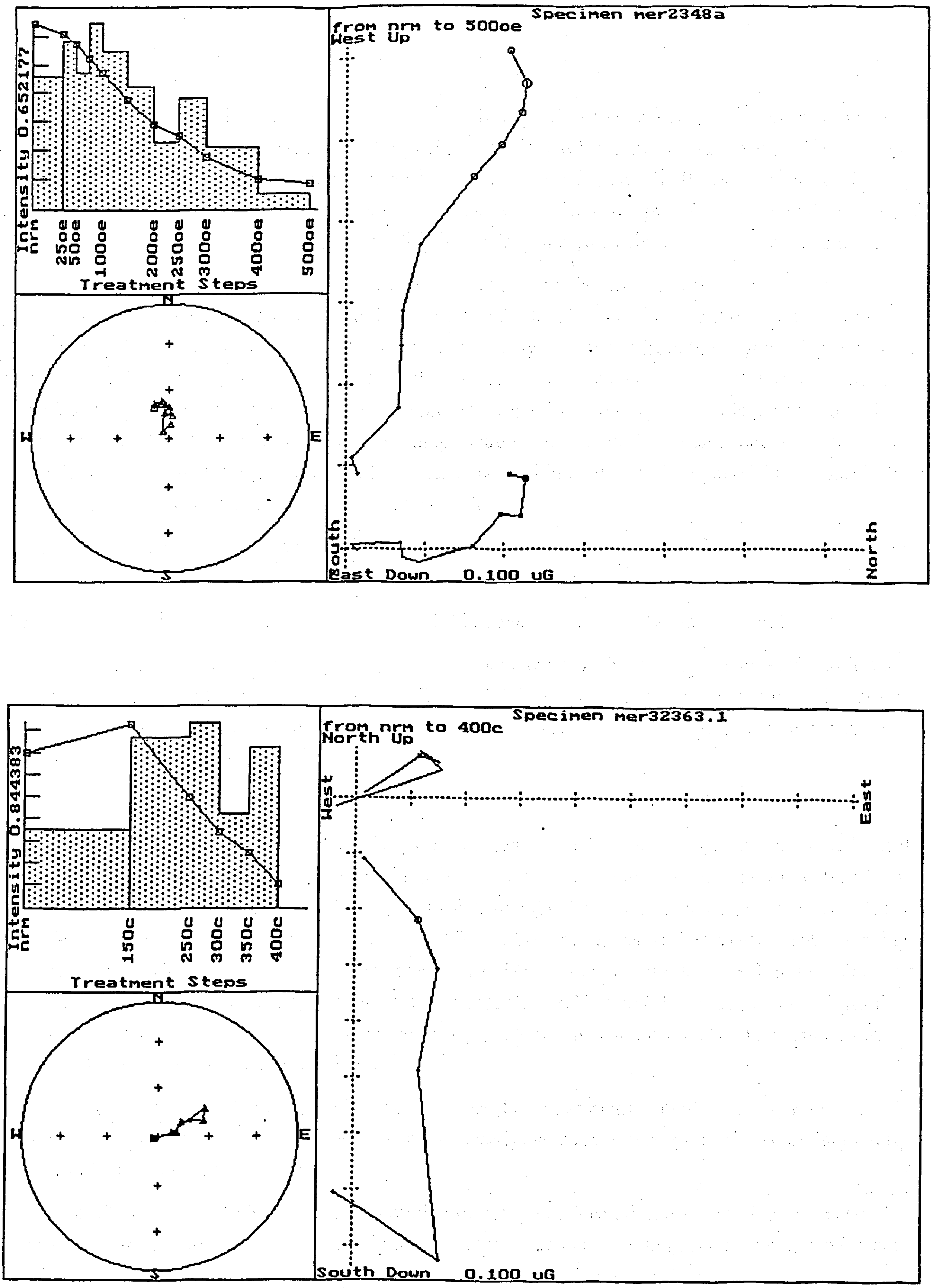

Figure 5.2 Intensity plot, stereographic and orthoganol plot of thermal and AF demagnetisation of selected specimens from above and below the negative $\delta^{13}C_{org}$ excursion in Merrimelia 3 borehole. The specimen identification is shown above the orthogonal plot and consists of the abreviation "mer" and the depth of the sample in metres. Intensity is in µG (mA/m). Treatment steps are indicated on the x axis of the intensity plot. In the stereographic plot, closed symbols indicate the lower hemisphere, open symbols the upper.

5.4 Discussion

The end of the Kiaman Reversed Superchron is marked by the onset of mixed polarity, above the Illawarra Transition. The Illawarra Transition, originally defined from the normal polarity found in the "Narrabeen Chocolate Shale" (= Patonga Claystone) at Stanwell Tops on the Illawarra coast south of Sydney (Irving and Parry, 1963), is now interpreted as a Cretaceous overprint (Embleton and McDonnell, 1980). The transition onset in Eastern Australian basins is obscured by the Cretaceous overprint.

In Merrimelia-3 the magnetic polarity reversal about the Permian-Triassic boundary may represent the transition from the Kiaman Reversed Superchron in the *Weylandites* Zone to the Illawarra Mixed Chron in the *P. microcorpus* Zone (Fig. 5.1) or, alternatively the change from the Kiaman Superchron to the Illawarra Transition may have occurred in the condensed sediments or lacuna between the limiting Stage 3 and Upper Stage 5 samples. With no representation of intervening zones it is possible that the early Illawarra Mixed Chron normal polarity samples are not preserved in the sequence. If so the samples above the base of Upper Stage 5 represent samples deposited in a reversed interval of the Illawarra Mixed Chron. A number of points should, however, be noted:

1) The zone of reversed magnetic polarity extends above the sample of the *Weylandites* Zone (Kemp et al., 1977).

2) All samples in Upper Stage 5 from Merrimelia-3 have reversed magnetic polarity, and

3) The first sample with normal magnetic polarity is above the negative $\delta^{13}C_{org}$ excursion and lies above the single sample identified as *P. microcorpus* Zone (G. Woods pers. comm, 1993) within an interval where attempts to obtain a palynological determination have proven unsuccessful (G. Woods pers. comm., 1993, shown in Table 2.24).

5.5 Conclusions

The results of this combined $\delta^{13}C_{org}$ / paleomagnetic study of the Cooper Basin – Late Permian reversed polarity below the $\delta^{13}C_{org}$ excursion with normal polarity above – is similar to the results of studies of the Permian-Triassic boundary at Shangsi, China (Heller et al., 1988; Steiner et al., 1989; Sweet et al., 1992, fig 1.2) (Fig. 5.3), Gartnerkofel Core (GK-1), Austria (Zeissl and Mauritsch, 1991, fig. 12) (Fig. 5.4), South China at Shuijiang, Wulong and Linshui (Heller et al., 1995), and Salt Range, Pakistan (Haag and Heller, 1991), and supports the assertion of Haag and Heller (1991, p. 53) that the Permian-Triassic boundary as indicated by the negative $\delta^{13}C_{org}$ excursion is situated close to a change from reversed to normal polarity, exemplified by:

1) Shangsi: The *changsingensis* conodont zone (latest Permian) is predominantly reversed polarity ending with a negative $\delta^{13}C_{CO3}$ excursion and the overlying *Isacica* Zone (Triassic) is predominantly normal polarity (Sweet et al., 1992).

2) Gartnerkofel-1 Core: The Late Permian Bellerophon Formation is predominantly reversed polarity ending with an interval of normal polarity in the latest Permian that coincides with a negative $\delta^{13}C_{CO3}$ excursion about the Permian-Triassic boundary (Zeissl and Mauritsch, 1991).

3) Salt Range: The upper Chhidru Formation is predominantly reversed with a short normal interval near the top of unit 4 of the Chhidru Formation (Haag and Heller, 1991, fig. 7).

4) Shuijiang, Wulong, and Linshui: The end Permian is associated with a change from a reversed to a normal polarity interval (Heller et al., 1995).

In Merrimelia-3, as found elsewhere, the negative $\delta^{13}C_{org}$ excursion about the Permian-Triassic boundary coincides closely with a reversed to normal magnetic polarity change. This consistent coincidence supports the primary nature of the $\delta^{13}C_{org}$ excursion in Merrimelia-3 and its correlation to the Permian-Triassic boundary.

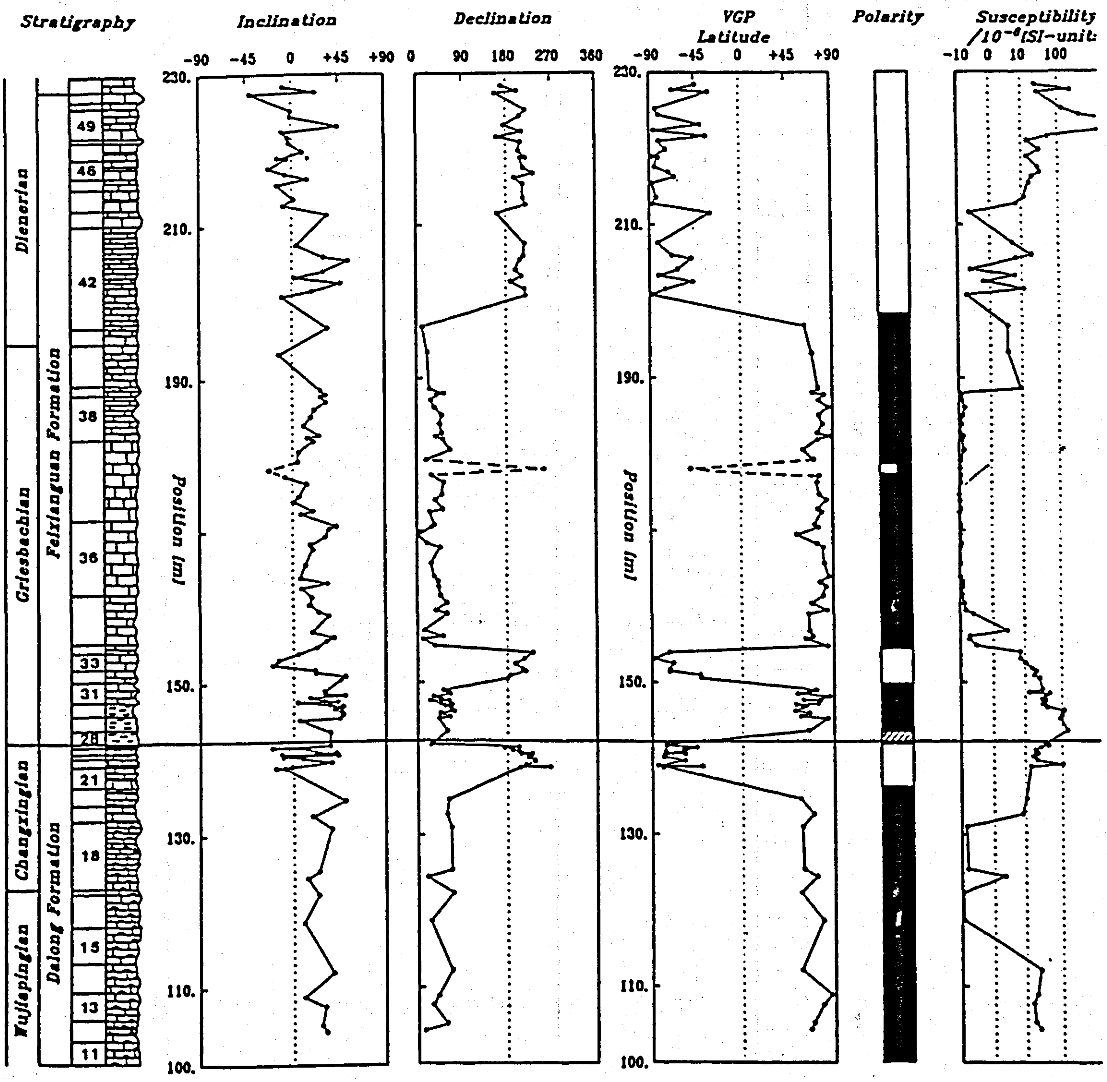

Figure 5.3 Magnetic polarity and $\delta^{13}C_{CO3}$ profiles about the Permian-Triassic boundary at Shangsi (Heller et al., 1988).

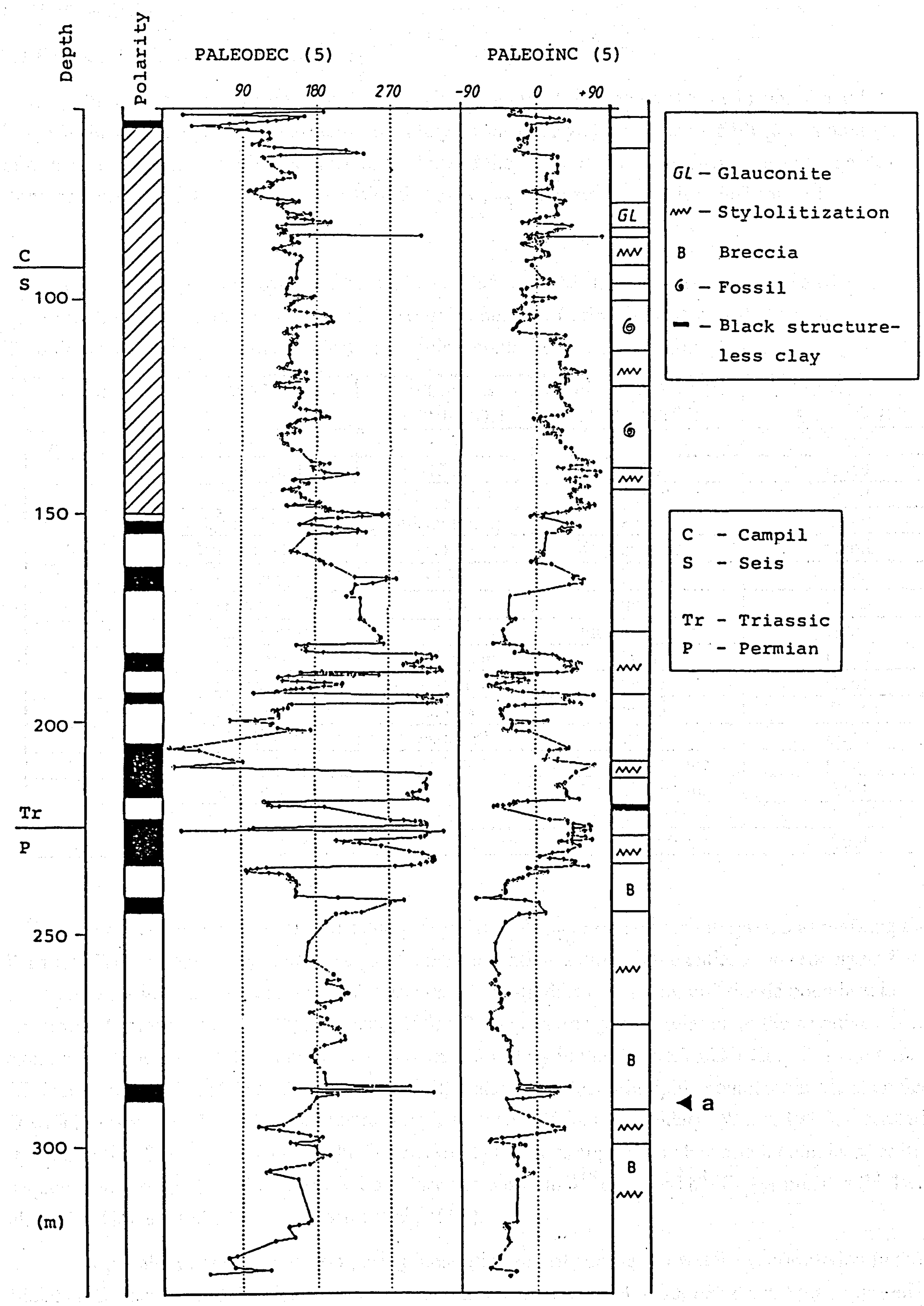

Figure 5.4 Magnetic polarity profiles about the Permian-Triassic boundary in Gartnerkofel-1 core from Zeissl and Mauritsch (1991).

6. SYNTHESIS

6.1 Carbon isotope results: Summary

Studies of organic carbon in whole-rock, fine-grained sediments obtained from boreholes in Australian marine and nonmarine sedimentary basins have yielded negative $\delta^{13}C_{org}$ excursions of 4 to 10‰ beginning within or close to the base of the miospore *Protohaploxypinus microcorpus* Zone of Helby et al. (1987). The results of this $\delta^{13}C_{org}$ study are summarised in Table 6.1.

Table 6.1 Summary of the key sections studied to define the $\delta^{13}C_{org}$ excursion, interpreted environment of deposition at the Permian-Triassic boundary (unless indicated as Permian or Triassic only), and the quality of biostratigraphical control based on palynology.

BASIN	WELL	δ^{13}Corg ‰ EXCURSION	ENVIRONMENT OF DEPOSITION	PALYNOLOGY CONTROL
Bonaparte	Tern- 3	-10 ‰	Marine	Good
	Fishburn-1	-10 ‰	Marine	Good
	Petrel-4	-4 ‰ to -8 ‰	Paralic?	Good
	Sahul Shoals-1	indeterminate	Marine	Spot
Canning	Paradise Cores	-8.5 ‰	Marginal marine	Good
Carnarvon	Onslow -1	-4 ‰	Marine	Spot
Bowen	Denison NS-20	-6 ‰	Fluvial	Good
	Eddystone-1	-4 ‰	Fluvial/marine	Good
	Taroom-10	Permian only	Marine	Good
	Eddystone-5	Permian only	Marine	Good
Perth	Whicher Range-1	-5.5 ‰	Fluvial	Spot
	BMR -10	Triassic only	Marine	Good
Sydney	Murrays Run-1	-5.5 ‰	Fluvial/lacustrine	Good
	Lisarow-1	-4 ‰	Fluvial/lacustrine	Spot
	Bunnerong-1	-8 ‰	Fluvial/lacustrine	Spot
	Newvale-28	? -3 ‰	Fluvial/lacustrine	Spot

The base of the interval of the sharp negative $\delta^{13}C_{org}$ excursion is interpreted as marking the Permian-Triassic boundary. The $\delta^{13}C_{org}$ excursion continues through the entire *P. microcorpus* Zone in Australian sedimentary basins so *P. microcorpus* Zone straddles the Permian-Triassic boundary in Australia (Morante et al., 1994; Retallack, 1995). This is based upon correlation to the negative $\delta^{13}C$ excursion at the paleontological Permian-Triassic boundary in the Gartnerkofel-1 Core from Austria (Holser et al., 1989; 1991; Magaritz et al., 1992) and the eventostratigraphic boundary at Meishan Section D which lies within 30 cm of the biostratigraphic Permian-Triassic boundary (Wang, 1995). Correlation of the Australian $\delta^{13}C_{org}$ profiles to the Gartnerkofel -1 Core is appropriate because it contains a continuous sequence across the Permian-Triassic boundary and has both $\delta^{13}C_{org}$ and $\delta^{13}C_{CO3}$ profiles (Holser et al., 1989; Holser et al., 1991; Magaritz et al., 1992).

A problem occurs when comparing biostratigraphical correlation and $\delta^{13}C$ correlation in the Meishan D Section and the Gartnerkofel-1 Core. In the Gartnerkofel-1 Core *H. parvus* the proposed Permian-Triassic boundary index fossil first occurs prior to the isotope minimum (Fig.1.7) whereas in the Meishan D Section the $\delta^{13}C$ excursion minimum occurs before the first appearance of *H. parvus* (Fig. 1.6). Assuming isochroneity of the $\delta^{13}C$ excursion minimum this indicates the incoming of *H. parvus* is delayed in Meishan D Section. The $\delta^{13}C$ excursion occurs over about 50 m in the Bonaparte Basin (Figs

2.3, 2.5) and contains the entire *P. microcorpus* Zone. Assuming the $\delta^{13}C$ excursion minima are all isochronous this implies that the time interval by which the incoming of *H. parvus* is delayed in the Meishan D Section is of the order of the *P. microcorpus Zone.*

Because the negative excursion is detectable in $\delta^{13}C$ profiles in nonmarine as well as marine sediments it can be used to correlate the Permian-Triassic boundary in differing environments of deposition (Morante et al., 1994; Morante and Herbert, 1994; Faure et al., 1995). The similarity in the $\delta^{13}C$ profiles of marine and nonmarine sections suggest the role of atmospheric carbon dioxide is pivotal in the equilibration of carbon isotopes across marine and nonmarine environments.

$\delta^{13}C_{org}$ values are around -24.5‰ in the marine and nonmarine Late Permian and as negative as –34.5‰ in the earliest Triassic of Australian sedimentary basins. These extremely negative $\delta^{13}C_{org}$ values are followed by an extended period beginning in the Early Triassic where the $\delta^{13}C_{org}$ values are around -27 to -30‰.

The $\delta^{13}C$ excursion (= Permian-Triassic boundary) coincides with a change in magnetic polarity from a reversed interval to a normal interval in the Cooper Basin, Australia. This is similar to the magnetic stratigraphy about the Permian-Triassic boundary in the Gartnerkofel-1 Core, Austria (Zeissl and Mauritsch, 1991) and China (Haag and Heller, 1991; Heller et al., 1995).

Permian $\delta^{13}C_{org}$ values below the negative $\delta^{13}C_{org}$ excursion in the marine Bonaparte and Canning Basins are generally more positive than those from time-equivalent intervals as correlated by palynological zones in the marine Bowen Basin. This may reflect a latitudinal gradient and be due to lower water temperatures in the Eastern Australian Basins that were closer to the pole during the Late Permian (Lackie and Schmidt, 1993). Lower water temperatures allow an increased amount of CO_2 to dissolve in the water and this results in more negative $\delta^{13}C_{org}$ values (Rau et al., 1989).

The negative $\delta^{13}C_{org}$ excursion occurs at the cessation of coal measures deposition in Eastern Australia (Morante et al., 1994; Veevers et al., 1994) and hence the change from coal measures to barren measures coincides with the Permian-Triassic boundary.

Glossopteris survived to within 50 cm of the hiatus at the Newcastle Coal Measures/Narrabeen Group boundary in the Sydney Basin in Murrays Run-1 corehole. This is 4.6 m after the beginning of the negative $\delta^{13}C_{org}$ excursion, within palynological zone Upper Stage 5, but lies around 20 m above the last coal (Morante and Herbert, 1994, figs 2, 3).

The Permian-Triassic boundary $\delta^{13}C$-excursion occurs at the Cherrabun Member/ Blina Shale boundary in the Paradise Cores in the Canning Basin (Morante et al., 1994) although the sharpness of the excursion and lithological evidence suggests the contact is a disconformity. This interpretation is supported by the thin (maximum depth of section = 6 m in Core # 4) *P. microcorpus* Zone (Fig. 2.10).

The Permian-Triassic boundary $\delta^{13}C$-excursion was shown to occur above the Tern Sandstone of the Hyland Bay Formation in Petrel-4 (Fig. 2.4), at the top of the Tern Sandstone Member in the Tern-3 (Fig 2.3), and below the Tern Sandstone in Fishburn-1 (Fig. 2.5). Such a pattern is best explained by accepting the Tern Sandstone to be a near shore sand deposited during a regression. This is also supported by the apparent diachronous nature of the Tern Sandstone when compared to palynological zonations in Fishburn-1 and Tern-3.

During the Permian, $\delta^{13}C_{CO3}$ values determined from nonluminescent brachiopods are almost exclusively more positive than 4‰ (Table 4.2). The average $\delta^{13}C_{CO3}$ value for palynological zones

Upper Stage 4b, Lower Stage 5, and Upper Stage 5 is around 5‰, and for Upper Stage 4a it is around 6‰ (Table 6.2).

A positive $\delta^{13}C_{CO3}$ value of 5‰ or greater persisting until very late in Upper Stage 5 is suggested by the whole rock $\delta^{13}C_{CO3}$ values determined on the H4 Limestone from the Bonaparte Basin, northwestern Australia in Sahul Shoals-1 (5.6‰) and Petrel-4 (5.0‰). The H4 Limestone contains Chhidruan (= Djulfian) brachiopods in Sahul Shoals-1 (Archbold, 1988; Archbold pers. comm., 1995). Further support for the maintenance of very positive $\delta^{13}C_{CO3}$ values until the latest Permian comes from the studies of nonluminescent brachiopods from Sichuan, China where values that tend to become more negative up sequence range from 6.3 to 0‰ during the Changxingian (Gruszczynski et al., 1990). The lower time limit of the period of high $\delta^{13}C_{CO3}$ values is unclear from the Australian data however the positive $\delta^{13}C_{CO3}$ values of brachiopod calcite in palynological zone Stage 3 of Tasmania suggest at least the Early Permian (Rau and Green, 1983).

The $\delta^{13}C_{CO3}$ profiles established in parallel with the $\delta^{13}C_{org}$ profiles through the marine Late Permian of the Bowen Basin indicate a difference between the two values of around 30‰ (Figs. 2.21, 2.22, and 2.23).

Table 6.2 Carbon isotopes by palynology zone.

Palynology Zone	$\delta^{13}C_{CO3}$ ‰ range.	$\delta^{13}C_{CO3}$ ‰ average	n	σ ‰
Upper Stage 5	6.80- 2.36	5.2	10	1.2
Lower Stage 5	7.3- 4.25	5.0	5	1.2
Upper Stage 4b	7.35- 3.50	4.8	8	1.1
Upper Stage 4a	7.80- 4.40	6.3	25	1.0

Data from Early Triassic nonluminescent brachiopods is sparse hence there is a heavy reliance upon whole-rock limestone data from the Tethyan margin and South China regions (see Grossman, 1994; Baud et al., 1989). Because of this it is only possible to say that $\delta^{13}C_{CO3}$ appears to be around 0‰ in the Early Triassic although much more negative $\delta^{13}C_{CO3}$ values (eg. -6‰) have been recorded in the earliest Triassic (Xu and Yan, 1993; Chen et al., 1991).

The $\delta^{13}C$ value is dependent upon the proportion of carbon buried as organic carbon compared to the total amount of carbon buried in sediments (Knoll, 1991). The higher the amount of organic matter buried and preserved the more positive the $\delta^{13}C$ values (Fig. 1.3). This relationship suggests that a high proportion of carbon buried in the Permian was organic carbon and that the proportion of carbon buried as organic carbon was much lower in the Early Triassic. Support for a lower flux of organic matter being buried during the Early Triassic compared to the Permian comes from the generally decreased TOC of samples analysed above the negative $\delta^{13}C$ excursion compared to those below the excursion.

Because the organic matter preserved about the Permian-Triassic boundary can be assumed to be primarily of a plant origin the factors that affect the $\delta^{13}C$ of plants should be considered in terms of their ability to change the $\delta^{13}C$ of organic carbon buried. Factors known to affect the $\delta^{13}C$ of plants are listed below.

Factor	Affect
$\delta^{13}C$ of ambient CO_2	Varies according to the $\delta^{13}C$ of CO_2
Low light	-5 to -6‰
Low nutrients	-3 to -5‰
High CO_2	-3 to -7‰
Osmotic stress	5 to 10‰
Aridity	3 to 6‰

(O'Leary, 1988; van der Merwe and Medina ,1991; Tieszen, 1991)

Because the $\delta^{13}C$ excursion about the Permian-Triassic boundary has been shown to be global and persistant, only those factors causing a global effect should be considered as possible causes of the $\delta^{13}C$ excursion observed in organic matter at the Permian-Triassic boundary. There is no evidence of continuous global aridity or osmotic stress causing factors operating during the Permian so the possibility that the Permian positive $\delta^{13}C_{org}$ values are the result of these factors can be disregarded. Global low nutrient levels on land and in the oceans producing negative $\delta^{13}C_{org}$ values about the boundary is also unlikely. Global low-light conditions might be possible through an association with explosive volcanism (Campbell et al., 1992) or bolide impact and therefore cannot be discounted, however, the negative excursion persists well into the Triassic and beyond evidence for continuous explosive volcanism. Elimination of these factors leaves a change in the CO_2 pressure. Evidence exists for warming at the Permian-Triassic boundary in the change in $\delta^{18}O_{CO3}$ (Holser et al., 1989; Bowen, 1992). This suggests an increase in the CO_2 pressures may have occurred and may have been the result of oxidation of ^{13}C-depleted carbon (Holser et al., 1989: Faure et al., 1995).

6.2 Implications of the $\delta^{13}C_{org}$ profiles for the Permian-Triassic timescale in Australia

The location of the negative $\delta^{13}C$ excursion confirms the traditional placement (David and Browne, 1950) of the Permian-Triassic boundary at the coal measures/barren measures boundary in Eastern Australia and conflicts with aternative placements of the boundary at the top of the *P. microcorpus* Zone (Helby et al., 1987) and at the *P. samoilovichii* Zone (Foster, 1982).

The *P. crenulata* and *Weylandites* Zones below the negative $\delta^{13}C$ excursion are concluded to be of latest Permian age. Similarly the *P. microcorpus* Zone immediately above the base of the negative $\delta^{13}C$ excursion is concluded to be earliest Triassic.

The age of the *P. microcorpus* Zone is confirmed to have an upper age limit of the base of Upper Griesbachian by the work of Summons et al. (1995), in the Perth Basin who confirm the $\delta^{13}C$ results of Morante et al. (1994) that very negative $\delta^{13}C_{org}$ values continue into the bivalve *C. stachei* Zone which is of Upper Griesbachian age. That zone is coincident in BMR-10 with the palynological *K. saeptatus* Zone which lies above the *P. microcorpus* Zone (or its equivalent) in other West Australian sedimentary basins.

6.3 Mass and $\delta^{13}C$ balance constraints for the Permian and Early Triassic

The average value of $\delta^{13}C$ of primary carbon from the Earth's interior, the probable average of $\delta^{13}C$ in the Earth's surficial reservoirs, is around -5‰ (Broecker, 1970; Holser, 1988). A portion of that carbon is buried as organic matter, which tends to be markedly depleted in the ^{13}C isotope due to kinetic isotope effects occurring during photosynthesis (Park and Epstein, 1960; Schidlowski and Aharon, 1992). This means that carbonates tend to be enriched in the ^{13}C isotope.

Only C3 plants existed during the Permian and Triassic therefore the degree of fractionation that could be expected between plants and carbonates during the Permian and Triassic was probably about –20‰ from that of the atmospheric CO_2.

The $\delta^{13}C_{org}$ values during the Permian in marine and nonmarine environments were around –24 to –25‰. If mass balance is to be maintained it is therefore necessary that the carbonates deposited during this time had $\delta^{13}C_{CO3}$ values more positive than –5‰ and the results of this study (Table 6.2) indicate values generally above 4‰. The relationship between organic carbon and carbonate carbon buried can be expressed as an isotope mass balance equation (Broecker, 1970; Schidlowski et al., 1983; Summons and Hayes, 1992; Karhu, 1993)

$$\delta_i = f_{org}\,\delta_{org} + f_{CO3}\,\delta_{CO3} \quad \text{(Eq. 1)}$$

δ_i is the average carbon δ imputed to the surficial system assumed at -5‰.

f_{org} is the fraction of total carbon buried that is organic matter.

δ_{org} is the average carbon isotope composition of that organic matter.

f_{CO3} is the fraction of total carbon buried that is carbonates.

δ_{CO3} is the average carbon isotope composition of those carbonates.

Total carbon buried is the total of $f_{org} + f_{CO3}$ and equals 1.

Substituting

$$f_{CO3} + f_{org} = 1$$

into

$$\delta_i = f_{org}\,\delta_{org} + f_{CO3}\,\delta_{CO3}$$

and denoting the difference between δ_{org} and δ_{CO3} as Δ and solving for f_{org} in Eq. 1 gives

$$f_{org} = (\delta_{CO3} - \delta_i) / \Delta. \quad \text{(Eq. 2)}$$

Assuming δ_i at -5‰ and substituting the average values of δ_{CO3} and Δ experimentally determined for each palynological zone of the Permian, the f_{org} for each Australian palynological zone where Δ pairs are known can be calculated from Eq. 2. These calculated values of f_{org} are listed in Table 6.3.

Table 6.3 Organic carbon burial by palynological stage.

Palynology zone	average δ_{CO3}‰	average Δ‰	Calculated f_{org}
Upper Stage 5	5.2	29.0 (n = 7)	0.35
Lower Stage 5	5.0	30.0 (n = 1)	0.33
Upper Stage 4b	4.8	28.9 (n = 6)	0.34
Upper Stage 4a	6.3	30.2 (n = 13)	0.37

The calculated Permian f_{org} values are remarkably constant and very high compared to values of f_{org} of 0.19 calculated for the Early Triassic assuming $\Delta = 27‰$ (Magaritz et al., 1992), $\delta_{CO3} = 0‰$ (Grossman, 1994), and $\delta_i = -5‰$. These calculated values of f_{org} imply a significant reduction in the fraction of organic matter buried during the Early Triassic compared to the Permian. This is supported by the general fall in TOC of sediments above the negative $\delta^{13}C_{org}$ excursion found in this study.

Although not a direct measure of productivity the f_{org} decline over the time interval from the Late Permian to Early Triassic when combined with lithological evidence such as the cessation of coal measures deposition is suggestive of a decline in global primary productivity.

6.4 Interpretation of $\delta^{13}C$ isotope profiles

Using the mass balance calculations it becomes possible to interpret the distinct segments A, B, C, and D of the $\delta^{13}C$ isotope profiles (Fig. 6.1).

Segment A of the $\delta^{13}C$-profiles is interpreted to represent the steady state flux of carbon in the Permian prior to the mass extinction event with an f_{org} of around 35%. The $\delta^{13}C_{org}$ of most samples from segment A is in the range -23 to -24.5‰.

The period of and immediately following the mass extinction is represented by segment B where the dramatic negative $\delta^{13}C$ excursion occurs during the earliest Triassic. Assuming that the extreme negative spike in $\delta^{13}C$ in carbonates of around -4‰ in China (Xu and Yan, 1993) and organic matter –34.5‰ (Morante et al., 1994) represented by the boundary between segments B and C of $\delta^{13}C$ -isotope profiles is a reflection of the primary record (with $\Delta = 28.5‰$) then by substituting into

$$f_{org} = (\delta_{CO3} - \delta_i) / \Delta \quad \text{(Eq. 2)}$$

the f_{org} over the time interval represented as segment B on the $\delta^{13}C_{org}$ profiles can be calculated to show f_{org} may have reached a level as low as 0.04 at the extreme minimum in the $\delta^{13}C_{org}$ profiles. The proportion of carbon buried as organic carbon at the time of extreme negative values of -34.5‰ might have been negligible at around 4 %.

Segment C is interpreted to represent a phase following the extinction event where $\delta^{13}C$ values return to more positive values as f_{org} increased. This shift to more positive $\delta^{13}C$ values may represent a time of formation of a stratified ocean with large amounts of ^{13}C -depleted carbon stored below a redoxcline. This may be indicated by the poorly time constrained positive cerium anomaly that indicates marine anoxia detected in Scythian conodonts from Utah and Nevada, USA (Wright et al., 1987). The cerium anomaly is constrained to occur between the Late Guadalupian and Late Scythian. Anoxia could be associated with a stratified ocean which in turn could result in enhanced storage of ^{13}C -depleted carbon stored below a redoxcline hence resulting in an increase in $\delta^{13}C$ values in surface waters. The only positive excursion in $\delta^{13}C$ values of any significant time length is that occuring after the Permian-Triassic boundary during segment C of the $\delta^{13}C$ isotope profiles. Alternatively this segment may represent the establishment of a new biotic regime when f_{org} increased as new biomes were established and there was a return to higher levels of primary productivity after the mass extinction. The global Early Triassic coal gap does not, however, support such a regime having been re-established (Faure et al., 1995; Retallack et al., in press).

Segment D is interpreted to represent a new Early Triassic steady state that reflects a lowered f_{org} than that occurring during during the Permian of around 20% of total carbon burial. The $\delta^{13}C_{org}$ of samples from segment D is generally in the range -27 to -30‰.

The residence time of carbon in the ocean-atmosphere reservoir is on the order of 200 000 to 140 000 years so the carbon isotope composition for materials entering the sedimentary reservoirs must be identical to the carbon added to the ocean-atmosphere by chemical weathering and earth degassing on a scale greater than 200 000 to 140 000 years (Broecker and Woodruff, 1992; Walker, 1986). A sudden catastrophic oxidation of ^{13}C-depleted carbon could therefore cause disruption of the surficial reservoirs of carbon for a period approaching 200 000 years before being purged from the system. Since any catastrophic release or oxidation of ^{13}C-depleted carbon would probably occur over a period of time rather than instantaneously it would be reasonable to conclude that there would be a decrease/increase cycle in $\delta^{13}C$ values in both carbonate and organic carbon similar to that observed in $\delta^{13}C$ profiles about the Permian-Triassic boundary (segments B and C). By similar reasoning, the minimum timespan of segment C is therefore on the order of 200 000 years assuming it represents only a recovery phase when no additional disruptive catastrophic releases of ^{13}C-depleted carbon occurred and that the isotope values finally achieved are representative of a steady state.

The timespan of segment B is somewhat more complex but an extended period is suggested by the gradual nature of the ^{13}C-depletion in interpreted complete sections and it is probably of the order of 10^5 or more years.

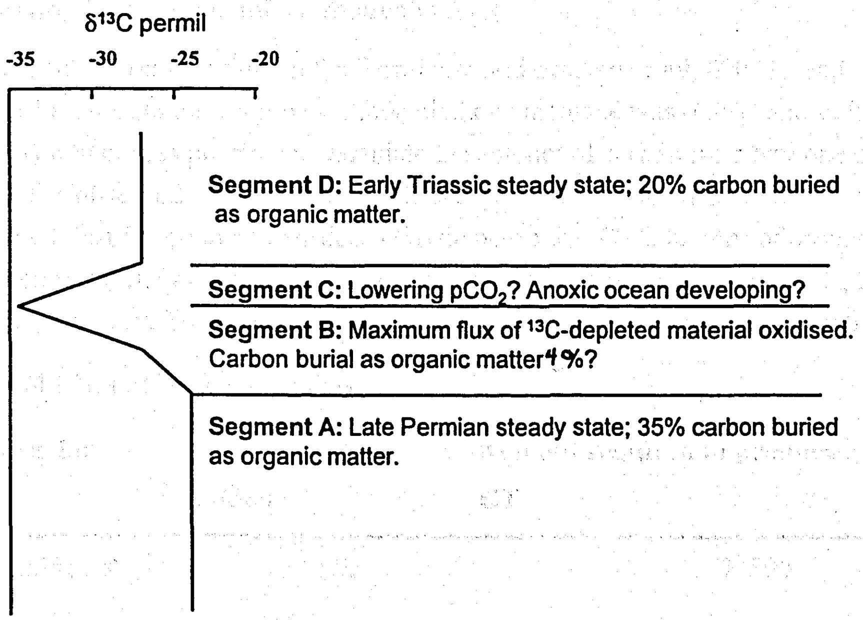

Figure 6.1 Interpretation of carbon isotope profile segments.

6.5 The Permian-Triassic $\delta^{13}C$ excursion - implications for the flux rates of carbon between reduced and oxidised reservoirs

Estimates of the amount of carbon from different sources required to produce a shift in $\delta^{13}C$ values can be calculated using the equation of Spitzy and Degens (1985). This equation assumes rapid mixing and ignores feedback mechanisms but does give an idea of the transfer of carbon between various reservoirs.

$$N_B = N_A * \frac{(1+R_B) * (R_A - R_M)}{(1+R_A) * (R_M - R_B)}$$

Where

N_A = Size of reservoir A

N_B = Size of reservoir B

R_A = Ratio of isotopes in reservoir A

R_B = Ratio of isotopes in reservoir B

R_M = Ratio of isotopes in mixed reservoirs A+B

Assuming the amount of DIC in the Permian world ocean was 40, 000 GT and the $\delta^{13}C_{PDB}$ value of organic matter in the Late Permian was -25‰; clathrate methane was -65‰; and volcanic gases was -5‰ (Erwin, 1993) it becomes possible to calculate the amount of carbon from any one of these reservoirs that would cause the observed $\delta^{13}C$ shift from +2‰ to -8‰, the assumed Dissolved Inorganic Carbon or DIC values for the latest Permian and earliest Triassic ocean. $\delta^{13}C$ excursions of around -10‰ are observed in carbonates (Xu and Yan, 1993) and confirmed in organic carbon (Figs 2.3, 2.6) about the Permian-Triassic boundary. The results of the calculations are tabulated below (Table 6.4).

Table 6.4 Mass balance constraints.

Source of carbon added	**$\delta^{13}C$ of carbon added**	**Amount required to produce a -10‰ shift GT**
methane clathrates	-65‰	7, 500
organic matter	-24‰	25, 000
volcanic gases	-5‰	133, 000

From these calculations and considering the volumes of various carbon reservoirs in the global carbon reservoir today listed in Table 6.5 as a close proxy for the Late Permian, it is possible to speculate on the possible source of the carbon that produced $\delta^{13}C$ excursion. It is obvious that since a contribution from the carbonate reservoir would affect the $\delta^{13}C$ very little if at all because it is approximately at the Late Permian value of 2‰ (or would have been more positive from the results determined using nonluminescent brachiopods and whole rock limestones herein with values generally above 4‰) that the carbonate reservoir did not contribute to the excursion. Because of the huge volume of mantle required to produce a –10 ‰ excursion it is unlikely that volcanic eruption alone produced the excursion. The only viable single sources of carbon capable of producing a change of -10‰ across the Permian-Triassic boundary, assuming a nonstratified ocean, are hence organic matter from sediments or methane from clathrates (Morante, 1993b; Erwin, 1993; Morante et al., 1994). The likelihood is, however, that the ^{13}C-depleted carbon that caused the $\delta^{13}C$ excursion came from multiple sources rather than a single source.

Table 6.5 Carbon reservoirs today (Erwin, 1993).

Reservoir	Amount in GT approx.
Carbonate sediments	6,000,000
Organic carbon in sediments	1,300,000
Gas hydrates	10,000
Dissolved organics in the oceans	1000
Oil, gas, and coal	5000
Humus, peat, and detritus	2000
Land biota	800
Marine biota	3
Atmosphere	700

6.6 $^{87}Sr/^{86}Sr$ results summary

Analysis of the $^{87}Sr/^{86}Sr$ determined from 33 nonluminescent brachiopod shells mainly from the Spiriferacea and Productacea from Australian sediments of late Early to latest Late Permian based on palynological biostratigraphical schemes (Price, 1983) has revealed a precipitous fall in $^{87}Sr/^{86}Sr$ values from about 0.70720 in sediments of palynological zone Lower Stage 4 to a minimum value of 0.70647 during the Upper Stage 5 Zone. The minimum $^{87}Sr/^{86}Sr$ recorded in GSQ Eddystone-5 at 735 m occurs in a sequence where V. Palmieri (pers. comm., 1992) has identified Kazanian foraminifera.

Following the minimum $^{87}Sr/^{86}Sr$ (which is the lowest reported in the Phanerozoic) at the Ingelara/Peawaddy boundary, a rapid rise in $^{87}Sr/^{86}Sr$ occurs in calcite samples from sediments stratigraphically higher in the Peawaddy Formation to 0.70695. The $^{87}Sr/^{86}Sr$ minimum therefore is concluded to occur about the topmost Ingelara /basal Peawaddy Formation in GSQ Eddystone-5. Calcite from a brachiopod at 647 m in GSQ Eddystone-1 within the Peawaddy Formation and interpreted to be younger (because of relative stratigraphic position) than the sample from the top Ingelara Formation in Eddystone-5 has a $^{87}Sr/^{86}Sr$ of 0.70693. Samples lower in the section than the Ingelara/ Peawaddy boundary in GSQ Eddystone-1 at 692 to 947 metres show a general trend towards increasing $^{87}Sr/^{86}Sr$ with increasing depth.

A brachiopod calcite sample from the topmost Peawaddy Formation within the Mantuan Productus beds in GSQ Springsure-19 corehole at 514.25 metres has a $^{87}Sr/^{86}Sr$ of 0.70689 supporting a conclusion that the inflection point of the Late Permian minimum $^{87}Sr/^{86}Sr$ is around the topmost Ingelara Formation or basal Peawaddy Formation.

In all corehole sections or outcrop samples analysed from the Bowen Basin there is a trend for a decline in the $^{87}Sr/^{86}Sr$ to a minimum at the top Ingelara Formation/ basal Peawaddy Formation whereafter the $^{87}Sr/^{86}Sr$ rises.

A brachiopod calcite sample from the Djulfian Cherrabun Member, Liveringa Group, Canning Basin, has a $^{87}Sr/^{86}Sr$ of 0.70716 supporting the continuation of this trend of increasing $^{87}Sr/^{86}Sr$ up section approaching the Permian-Triassic boundary.

The $^{87}Sr/^{86}Sr$ seawater ratio at any particular time in the Phanerozoic is thought to be a function of riverine Sr flux (controlled by orogenic uplifting and major glaciations) that tends to have a high $^{87}Sr/^{86}Sr$, and hydrothermal input from submarine volcanism that tends to have a low $^{87}Sr/^{86}Sr$. At any time the balance between the riverine input and hydrothermal input to the oceans is reflected in the seawater $^{87}Sr/^{86}Sr$ determined from well preserved carbonates (Denison et al., 1994). A decrease in the proportion of hydrothermal input of Sr compared to riverine input of Sr will therefore result in an increase in the $^{87}Sr/^{86}Sr$ in seawater.

The fall in the $^{87}Sr/^{86}Sr$ during the Early to Middle Permian represents a dominance of hydrothermal $^{87}Sr/^{86}Sr$ inputs over riverine $^{87}Sr/^{86}Sr$ inputs which continues until within the Upper Stage 5 Zone. This dominance of hydrothermal $^{87}Sr/^{86}Sr$ inputs over riverine inputs is somewhat surprising considering the end of major glaciation occurred during the Asselian (Dickins, 1993) and this could be expected to result in isostatic rebound of continents and a major flux of riverine $^{87}Sr/^{86}Sr$ to the oceans.

The $^{87}Sr/^{86}Sr$ seawater curve fall and rise from a minimum during the Late Permian (Denison et al., 1994) is paralleled by the results from Australian samples. It is therefore possible to use the $^{87}Sr/^{86}Sr$ minimum for correlation and conclude that the Guadalupian/Ochoan boundary lies within Australian palynological zone Upper Stage 5.

This is interpreted as indicating that hydrothermal activity in the oceans was waning from the Late Permian Ochoan/Guadalupian boundary as the seawater $^{87}Sr/^{86}Sr$ begins a rapid rise from about the Guadalupian/Ochoan boundary which continues beyond the Permian-Triassic boundary. This conclusion is supported by eustatic models (Holser and Magaritz, 1987; Ross and Ross, 1987) that indicate sealevel falling in the Late Permian and supports a model of subduction and seafloor spreading rate decline associated with the assembly of Pangea (Schopf, 1974). Such a decline would produce an overall increase in the depth of the ocean basins as the mid ocean ridge profile contracted due to isostatic loading of cooler, denser crust in the ocean floor more proximal to the ridge (Schopf, 1974). The assembly of Pangea should also produce a shorter mid-ocean ridge (Veevers, 1994) that would also result in lowered hydrothermal activity and a greater ocean basin volume. The $^{87}Sr/^{86}Sr$ seawater curve therefore supports a greater ocean volume having developed during the Latest Permian. The lower sealevel would then enable some isostatic adjustment of shelf margin sediments enhancing the effect of a sealevel fall.

6.7 Implications for the Australian Permian timescale

The $^{87}Sr/^{86}Sr$ minimum occurs within Upper Stage 5 therefore Upper Stage 5 base has a minimum age of Guadalupian. The negative $\delta^{13}C$-excursion that marks the Permian-Triassic boundary lies some hundreds of metres up section from the $^{87}Sr/^{86}Sr$ minimum so the $^{87}Sr/^{86}Sr$ minimum precedes the boundary by a time interval of several million years.

Upper Stage 5 palynological Zone spans a time interval at least part way through the Guadalupian to the Permian-Triassic boundary as it is constrained by the $^{87}Sr/^{86}Sr$ minimum above its base and the negative $\delta^{13}C$-excursion at its top. This provides some indication of the Upper Stage 5 megaflora's stability spanning much of the Late Permian and contrasts with its rapid, but not instantaneous, demise (Foster, 1982) coinciding with the $\delta^{13}C$-excursion.

6.8 Synopsis

The $\delta^{13}C$ excursion enables correlation across marine and nonmarine environments of deposition in Australian sedimentary basins.

The size of the $\delta^{13}C$ excursions in both carbonate (Xu and Yan, 1993) and organic carbon (Morante et al., 1994) of up to 10‰ exceeds that which can reasonably be explained by a fall in primary productivity alone (Spitzy and Degens, 1985; Gruszczynski et al., 1989). Of the alternative sources for ^{13}C-depleted carbon that might have caused the excursion, oxidation of a combination of organic carbon in sediments (Holser et al., 1989; Faure et al., 1995) and methane from clathrate deposits appears most likely (Erwin, 1994; Morante, 1993b; Morante et al., 1994; Summons et al., 1995).

The case for methane contributing to producing the observed $\delta^{13}C$ excursion is supported by a) the very negative $\delta^{13}C$ values of clathrate methane (Kvenvolden, 1993) which are generally less than –60‰ so that a lesser quantity of carbon is required to produce the observed $\delta^{13}C$-isotope excursion of up to –10‰, b) the strong greenhouse effect of methane which is estimated to be about 25 times the forcing expected from CO_2 (Wahlen, 1993), and c) the potentially huge reserves of methane estimated to exist in continental polar areas and continental shelf sediments today (Kvenvolden, 1988; 1993) and could reasonably be expected to have existed in the Late Permian.

Methane clathrates are stable at conditions below 0°C and depths of 150 m in polar continental areas and at water depths below 300m on continental shelves where water temperatures approach 0° C (Kvenvolden, 1993). Evidence indicates a sea level fall (Holser and Magaritz, 1987; Ross and Ross, 1987) and warmer temperatures in the Late Permian approaching the Permian-Triassic boundary (Holser et al., 1991; Dickins, 1993; Faure et al., 1995). At the boundary in Gartnerkofel Core-1, the $\delta^{18}O_{CO3}$ values indicate a temperature rise of around 5°C (Holser et al., 1991; Bowen, 1992).

The seawater $^{87}Sr/^{86}Sr$ minimum appears to be a global marker in marine carbonate sediments. The seawater $^{87}Sr/^{86}Sr$ minimum does not coincide with the $\delta^{13}C$ excursion but precedes it by several million years. This precludes a direct association of the seawater $^{87}Sr/^{86}Sr$ minimum and the Permian-Triassic boundary extinctions but allows the seawater $^{87}Sr/^{86}Sr$ minimum to be associated with a chain of events during the Late Permian that may have led to the Permian-Triassic mass extinction.

The extreme negative values (< -33‰) in the $\delta^{13}C_{org}$ profile such as recorded in the Bonaparte, Canning and Perth Basins suggest very low ratios of carbon was buried as organic matter during the Early Triassic (f_{org} = 0.035). Such a value appears absurdly low especially considering that the formation of carbonate reefs during the Early Triassic was supressed leading to the "reef gap" during the Scythian (Flügel, 1994; Morante, 1993b) and the sparcity of Early Triassic limestones (Grossman, 1994).

The traditional view of the $\delta^{13}C_{org}$ value is that it is a direct function of the fraction of carbon buried as organic matter as opposed to carbonates (Knoll, 1991) (Figure 6.1). This condition only applies however when there is an equilibrium between carbon inputs and outputs to the surficial system or when net carbon burial as carbonates or as organic matter equals that entering the gaseous or ionic reservoirs as CO_2 or HCO_3^-.

In the case of catastrophic oxidation of organic carbon or methane with $\delta^{13}C$ as negative as -90‰ (Kvenvolden, 1993) the surficial reservoir may have been perturbed from equilibrium driving the $\delta^{13}C_{org}$ to values approaching those that would occur when the amount of carbon buried as organic matter is negligible. As a consequence of this it is more plausible to interpret the very negative $\delta^{13}C$ excursion about the Permian-Triassic boundary as reflecting a period of oxidation of sedimentary organic matter or methane that resulted in the amount of carbon being oxidised far outweighing the amount of carbon being fixed into either carbonates or organic matter for a brief time around the boundary interval. The net affect of such a flux of carbon to the oxidised global reservoir should be an increase in global temperature. That rise in temperature between the Permian and Triassic is confirmed by Karhu and Epstein (1986) in their analysis of $\Delta^{18}O$ values for phosphate-chert paired samples. The $\Delta^{18}O$ values for phosphate-chert paired samples enable paleotemperature calculations that are independent of the $\delta^{18}O$ values of the water in which the minerals formed so they potentially provide a more accurate reflection of temperature. Additionally because the oxygen isotopic signature from marine biogenic phosphate and phosphate-chert paired samples are parallel they are interpreted as representing a primary signature that indicates a temperature rise from the Permian to Triassic (Karhu and Epstein, 1986).

6.9 A model for events about the Permian-Triassic mass extinction

The faunal (Erwin, 1994) and recently recognised floral extinction in the transition from the Permian to the Triassic (Retallack, 1995; Morante et al., 1994) is the major mass extinction event in the Phanerozoic (Benton, 1995). Because the Permian-Triassic extinction is now recognised to have affected land biota (Morante et al., 1994, Retallack, 1995; Benton, 1995) and the magnitude of the negative $\delta^{13}C$ excursion at the Permian-Triassic boundary of up to 10‰ has been confirmed (Morante et al., 1994; Xu and Yan, 1993) a re-evaluation of the mechanisms causing the mass extinction is possible.

Different causes for the end-Permian extinction have been proposed. Table 6.6 reviews some of them and the effect they would have on the marine and nonmarine geochemical environment. Of course a number of mechanisms could have, and probably were, operating at the close of the Permian and could have contributed to the extinctions. Because the mass extinction is now known to have affected land biota as well as marine biota (Retallack, 1995) and some of the mechanisms are limited in their effect to only the marine realm they cannot explain the full extent of the mass extinction.

The timing of the extinction was probably gradual not sudden taking some millions of years rather than being a sudden catastrophe (Erwin, 1993; Teichert, 1988). This suggests that a long-term change affected environments about the Permian-Triassic boundary rather than a rapid "event". An attractive possibility is that a sudden loss of negative feedback mechanisms inhibiting environmental change were lost about the Permian-Triassic boundary.

The association of the $\delta^{13}C$ excursion and the mass extinction suggests a causal link between the biotic catastrophy and isotopic "event". As such the extinction mechanism also reflects a decline in organic carbon burial and as a proxy, primary productivity. A number of mechanisms outlined below would presumably affect diversity of species but should not reduce net primary productivity. These mechanisms cannot explain the isotopic record at the boundary.

Table 6.6 Extinction mechanism evaluation.

Suggested cause of extinction	Affects marine organisms	Affects nonmarine organisms	Rapid	Gradual	Reasons why not viable as a single extinction mechanism.	Explains isotopic data
Global cooling	✓	✓	?✓	✓	No clear evidence of ice in polar regions during the Latest Permian.	No. Oxygen data indicates warming (Karhu and Epstein, 1986; Bowen, 1992)
Oceanic anoxia	✓		✓		Evidence of the extinction affecting land biota now clear eg Retallack (1995); Benton (1995); no preservation of black shales.	No. May have occurred after the boundary.
Atmospheric anoxia.	✓	✓	?✓	✓	Large vertebrates survived the extintion event. This would not have been possible under extended anoxic conditions (Ruben,1992).	Yes.
Pyroclastic volcanism	✓	✓	✓		Other large scale eruptions have not caused mass extinction (Erwin, 1993).	Yes.
Flood basalt eruption	✓	✓	✓	?✓		Not as single cause but may have contributed.
Extra-terrestrial impact	✓	✓	✓		No clear evidence of shocked quartz, spherules or iridium anomaly typical of bolide impact.	Yes, negative excursion at the Cretaceous/Tertiary boundary.
Decline in provinciality	✓	✓		✓	Associated with the assembly of Pangea which had largely occurred up to 10 million years previously with little impact.	No. Decrease in number of species should not greatly affect biomass or carbon fluxes
Nutrient reduction	✓			✓	Evidence of the extinction affecting land biota now clear eg Retallack (1995); Benton (1995)	? Yes.
Salinity change	✓			✓	Evidence of the extinction affecting land biota now clear eg Retallack (1995); Benton (1995)	No should not dramatically affect isotopes.
Habitat diversity decrease	✓	✓		✓	Does not necessarily affect primary productivity.	No should not affect isotopes.
Species area effects	✓			✓	Evidence of the extinction affecting land biota now clear eg Retallack (1995); Benton (1995)	No affect on isotopes.
Trace element poisoning	✓			✓	Evidence of the extinction affecting land biota now clear eg Retallack (1995); Benton (1995)	No should not affect isotopes.

Adapting a model of climate change effected by methane (Fig. 6. 2A) (Kvenvolden, 1993) to encompass a tectonic cause for deepening ocean basins and hence sealevel fall at the Permian-Triassic boundary (Fig. 6. 2B) it is possible to predict how a catastrophic release of methane from clathrates may have occurred about the Permian-Triassic boundary and link a number of the features in the geological record. In the model shown in Fig. 6.2A climate is balanced by a methane cycle controlled by feedback mechanisms. The model shown in Fig. 6.2B shows how feedback mechanisms might fail in the methane cycle during times when the primary control over sealevel fall is nonglacial.

These features include: 1) $^{87}Sr/^{86}Sr$ seawater rise from a minimum during the Late Permian (Denison et al., 1994); 2) a major sealevel regression during the Late Permian culminating about the Permian-Triassic boundary (Holser and Magaritz, 1987); 3) warming over much of Pangea in the Late Permian (Dickins, 1992; Dickins, 1993) that is associated with high rates of CO_2 fixation by plants and deposition of carbonaceous shale and coal measures throughout much of Gondwanaland and China (Veevers et al., 1994). Removal of vast amounts of CO_2 in an environment where the hydrothermal flux was declining should result in a decrease in global temperature; 4) loss of Gondwanaland lakes (Yemane, 1993); 5) the lack of a Late Permian ice cap at polar latitudes (Dickins, 1993); 6) replacement of the Permian cool-temperate *Glossopteris* flora with Triassic warm, dry-adapted *Dicroidium* flora (Retallack, 1995); 7) the eruption of the Siberian Traps synchronous with the Permian- Triassic boundary within the estimated errors assigned to radiometric dates for both events (Cláoue-Long et al., 1991; Renne, 1995; Dalrymple et al., 1995); 8) the negative $\delta^{13}C$ excursion at the Permian-Triassic boundary; and 9) the transition of the Permian Laurasian submergent province to the emergent Laurasian province of the Triassic (Veevers, 1994).

The features of a possible, but by no means exclusive, scenario at the end Permian that may have led to the Permian-Triassic mass extinction, the cause or effect of the features, and evidence in the geological record for those features is listed in Table 6.7. This scenario closely follows one that was presented in a model (Fig. 6.3) by Erwin (1993) and Morante (1993b).

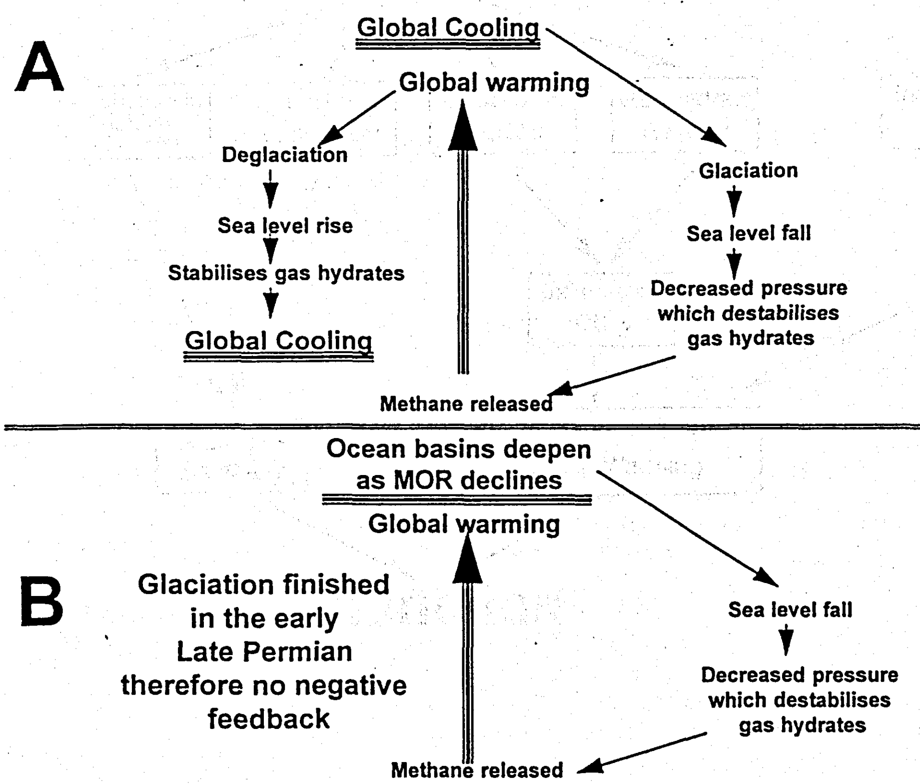

Figure 6.2 **A** is a modified Kvenvolden (1993) model showing how methane storage and release from clathrates moderates climate when eustatic level is controlled by glaciation through feedback mechanisms. **B Shows how this fails when** eustatic level is controlled by tectonics and leads to uncontrolled methane release and the potential development of a runaway greenhouse environment. Methane is an attractive source of ^{13}C-depleted carbon that potentially contributed significantly to the negative carbon isotope excursion about the Permian-Triassic boundary.

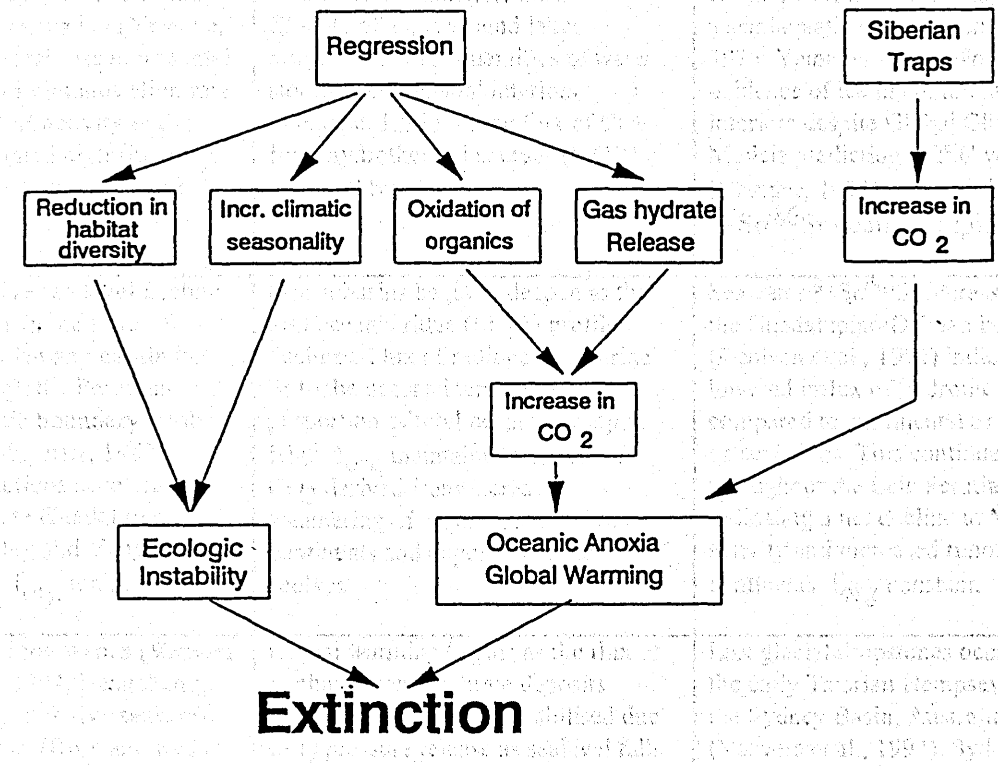

Figure. 6.3 Permian-Triassic mass extinction cause hypothesis from Erwin (1993, fig. 9.4)

Table 6.7 Permian- Triassic events.

Age	Feature	Cause/Effect	Evidence
Early to Mid Permian	Large Gondwanaland lakes established in the earlier Permian (Yemane, 1993) stabilise continental interior climates.High rate of MOR activity with associated high flux of non radiogenic Sr and CO_2.	Expanded habitat for *Glossopteris* in Gondwanaland interior basins. Climate of areas around lakes moderated. Huge quantities of water stored in continental interiors (Yemane, 1993). Large flux of CO_2 from hydrothermal sources (MOR) balanced by high f_{org}	Extensive *Glossopteris* biome. *Glossopteris* had roots adapted for a semiaquatic environment (Lele, 1976; Yemane, 1993). No evidence of ice in continental interiors despite Global Climate Models predicting -42° C winters (Yemane, 1993). f_{org} high. $^{87}Sr/^{86}Sr$ declines rapidly.
Late Permian	Relative sea level decline begins in the Late Kazanian and continues through the Permian-Triassic boundary (Holser and Magaritz, 1987). Extinctions accelerate in the Late Guadalupian (Stanley and Yang, 1994). High f_{org} maintained.	Ocean basins begin to deepen as the mid oceanic ridge (MOR) profile declines. Flux of radiogenic riverine Sr to the oceans increases as a proportion of total oceanic Sr input. High f_{org} maintained because of CO_2 derived from increased weathering of organic matter from continents and exposed marine shelves.	Seawater $^{87}Sr/^{86}Sr$ increases from the Guadalupian/Ochoan boundary (Denison et al., 1994) indicating lowered influx of hydrothermal Sr compared to continental Sr into the ocean basins. This continues throughout the Late Permian indicating a net decline in MOR activity and increased runoff from continents. f_{org} constant.
	Glaciation wanes (Veevers et al., 1994; Beauchamp, 1994). Relative sealevel declines (Ross and Ross, 1987).	Global warming begins as the flux of methane from clathrate deposits increases. Clathrates destabilised due to 1) pressure release as sealevel falls. 2) increased temperature in polar areas. A net transfer of continental reserves of water (remnant ice) to the ocean basins continues. Remnants of any ice sheets lost.	Last glacial dropstones occur in the early Tatarian Dempsey Fm of the Sydney Basin, Australia (Veevers et al., 1994). Sydney Basin at this time was close to or at polar latitudes (Lackie and Schmidt, 1993). High inclinations in Merrimelia 3 (this study, Fig. 2.33).
	Extensive Tatarian coal measures and carbonaceous sediments deposited in Gondwanaland and China (Veevers et al., 1994).	*Glossopteris* forest increases in southern Gondwanaland (Balme and Helby, 1973). The Cathaysia flora extensive in China (Faure et al., 1995). Increased burial of organic matter occurs in coal measures and carbonaceous shales. This removes most of the increased CO_2 flux from the atmosphere resulting from methane breakdown and limits greenhouse.	Gondwanaland coal measures sediments are found in Australia, India, South America, Antarctica, South Africa; widespread Chinese coal measures (Veevers et al., 1994). High C/S ratios during the Permian reflect limited pyrite formation in swamps and high rate of organic carbon burial on land compared to in the ocean (Berner and Raiswell, 1983, fig. 5). Glaciation not re-established despite large-scale organic carbon burial (up to 35 % carbon buried as organic matter).

Age	Feature	Cause/Effect	Evidence
Latest Permian	The transfer of water from continental reservoirs climaxes. Rapid net sealevel fall begins, the affect of minor sealevel cyclic falls on biota is magnified. Number of coal basins falls (Faure et al., 1995).	Continental shelf areas reduced, marine biota is stressed (Schopf, 1974). Moderate scale methane release from clathrates begins. The supply of hydroxyl radicals in the stratosphere and troposphere limits the breakdown of methane to CO_2 and water vapour (Wahlen, 1993). A major synergistic methane/CO_2 greenhouse is initiated.	Major sealevel regression about the Permian-Triassic boundary (Holser and Magaritz, 1987). $\delta^{13}C$ excursion begins. Mass extinction occurs on land and in the oceans. TOC of continental and marine sediments is reduced in the Early Triassic coinciding with reduced $\delta^{13}C$ values (Figs 2.3, 2.6, 2.10, 2.19, 2.20, 2.25, 2.27, 2.33).
?Permian - Triassic boundary	Siberian Traps erupt injecting a huge volume of SO_2 into the stratosphere (Campbell et al., 1992).	A brief SO_2 winter leading to ocean drawdown (Conaghan et al., 1994) which destabilises large marine shelf methane clathrate deposits as a result of pressure decrease. Large catastrophic methane release begins. A major synergistic methane/CO_2 greenhouse without a negative feedback mechanism begins.	$\delta^{13}C$ excursion accelerates at the boundary and rate of extinctions increases on land and in the oceans (Erwin, 1993; Retallack, 1995; Benton, 1995). Some evidence of permofrost structures in top coal measures in Eastern Australia indicating brief cooling about the Permian-Triassic boundary (Conaghan et al., 1994).
Earliest Triassic	Equator to poles thermal gradient is reduced. Thermohaline circulation and upwelling slows. Marine stratification increases and bioproductivity is greatly reduced similar to the current zooplankton decline associated with the warming of the California Current today (Roemmich and McGowan, 1995).	Nutrient recycling in the ocean slows, productivity declines in surface waters which have become warmer and therefore retain less dissolved gases. Dysaerobic conditions develop in shallow marine basins. Increased sulfide deposition occurs. Shelf organisms with high oxygen demands become extinct.	Increased level of sulfide deposits in sediments, surviving marine faunas are predominantly those requiring low levels of dissolved oxygen (Wignall and Hallam, 1992). Locally high f_{org} maintained in restricted basins eg. Perth Basin but generally f_{org} declined.
	The southern emergent (Gondwanaland) and northern submergent (Laurasia) hypsometric provinces of the Permian replaced by the single emergent Pangean province (Veevers, 1994).	Permian: Hypsometric provinces caused by unequal size of Pangea's original components. Triassic: Pangea assembly produced a supercontinent and the resultant self-induced heat anomaly plus deepening of the ocean basins led to a uniformly emergent Pangea (Veevers, 1994).	Permian: 15% Gondwanaland submergent, 25% Laurasia submergent. Triassic: Uniformly emergent Pangea. (Veevers, 1994).

6.10 Permian-Triassic timescale in Australia

With the publication of U/Pb SHRIMP ages for zircons from tuffs from several Permian formations in Eastern Australia (Roberts et al., 1994a; 1994b) combined with supplementary U/Pb SHRIMP ages that supersede Roberts et al. (1994a; 1994b; J. Roberts pers. comm., 1994), brachiopod zones amplified by Briggs, (1993b) and the location of the carbon isotope negative excursion (Chapter 2, isochronous at the Permian-Triassic boundary, and the $^{87}Sr/^{86}Sr$ minimum (Chapter 3) at the Guadalupian/ Ochoan boundary it is possible to reassess and derive a more tightly constrained Australian Permian and Triassic biostratigraphical and numerical timescale related to the global timescale. Derivation of that timescale (Figs. 6. 4, 6.5), is from the following markers:

1. The paleontological Permian-Triassic boundary in Meishan Section D, China marked by a negative carbon isotope shift within centimetres of the white Permian-Triassic boundary clay containing zircons with U/Pb ages 251± 3.4 Ma (Claoué-Long et al, 1991), now known to be topmost Permian because of the presence of Permian conodonts (Yin, 1993, p. 22) provides a numerical date. The 250 ±3.4 Ma (= 254.6 - 247.8 Ma) U/Pb SHRIMP date for the Black Alley Shale (Roberts et al., 1994a) between the $^{87}Sr/^{86}Sr$ minimum and the negative $\delta^{13}C$-excursion in Eastern Australia suggests that the Permian-Triassic boundary cannot be as old as the extreme 254.6 Ma indicated by the U/Pb SHRIMP date of 251.2± 3.4 Ma on a clay layer 30 cm below the Permian-Triassic boundary in the Chinese stratotype section, Meishan D (Claoué-Long et al., 1991). The Permian-Triassic boundary therefore has a maximum age of less than 253 Ma because the Black Alley Shale is overlain by the coal measures, the top of which is the Permian-Triassic boundary by correlation of the $\delta^{13}C$ excursion (Morante et al., 1994).

   Rb/Sr dates on biotites towards the top of the Blackjack Formation in the Gunnedah Basin of Eastern Australia give a mean maximum age of 251.1 Ma (Veevers et al., 1994). The Permian-Triassic boundary is therefore limited between 251.1 and 247.8 Ma. The Permian-Triassic boundary is therefore rounded at 250 Ma.

2. a) The Eastern Australian negative $\delta^{13}C$ excursion at the Coal Measures/Rewan/Narrabeen Group boundaries is correlated to the Permian-Triassic boundary at Meishan Section D (Xu et al., 1993) and Gartnerkofel-1 Core (Holser et al., 1991).

   b) Numerical dates for the latest Permian including the Rb/Sr ages of the top Blackjack Formation, Gunnedah Sub-basin of the Sydney Basin which cluster around 250 Ma (Veevers et al., 1994), the Awaba Tuff, Sydney Basin U/Pb bulk age of 256 ± 4 Ma (Gulson et al., 1992) and the three 250 ± 3 Ma U/Pb zircon SHRIMP ages of the Black Alley Shale, Bowen Basin (Roberts et al., 1994a; 1994b; J. Roberts pers. comm., 1994) indicate a latest Permian age for the terminal Sydney-Bowen Basin Coal Measures sedimentation.

   c) U/Pb zircon SHRIMP ages of 256 ± 3 Ma for the Condamine Beds, Silverwood Block, 257 ± 3 Ma ages for the Rhyolite Range, Silverwood Block, 264 ± 3 Ma for the Mulbring Formation, Sydney Basin, 274.1 ± 3.4 Ma for the Lakes Road Rhyolite (taken at central values), and 292 ± 5 Ma and 294 ± 5 Ma for the Alum Rock Conglomerate, Texas Woolomin Block (Roberts et al., 1994a; 1994b; Roberts pers. comm., 1994) averaged to 293 Ma provide markers through the Permian.

   d) The Ingelara Formation, Bowen Basin in GSQ Sprinsure 18 dates of 250 ± 3 Ma (from 435 m), 253 ± 3 Ma (from 480 m) and 263 ± 3 Ma (from 498 m) are ignored in this scheme because of the conflict in the 253 ± 3 Ma (from 480 m) and 263 ± 3 Ma (from 498 m) dates. The 250 ± 3 Ma (from

435 m) age is not accepted because of the conflicting stratigraphic position of the Ingelara Formation with respect to the Black Alley Shale with three dates about 250 ± 3 Ma.

3. Corresponding brachiopod and palynomorph zones related to the numerical dates available are plotted largely following Briggs (1993b) and Roberts et al. (1994a, fig. 1) as follows:

   a) The Blackjack Formation contains palynomorphs of Upper Stage 5c (Veevers et al., 1994, p. 192) and has a projected mean Rb/Sr age of 251.1 Ma.

   b) The Black Alley Shale is older than 251.1 Ma by projected superposition and I pick an age of 252 Ma (within 250 ± 3 Ma). Upper Stage 5c is projected to *Echinolosia* n.sp. G.

   c) The Condamine Beds date of 256 ± 3 Ma lies between *E.* n.sp. G and *E. ovalis* Zones and is equivalent to Upper Stage 5c.

   d) The Rhyolite Range date of 257 ± 3 Ma lies above *E. discinia.* This conflicts with the younger *E.* n.sp. D and *E.* n.sp. E Zones below.

   e) The Mulbring formation date of 264 ± 3 Ma lies between *E.* n.sp. D and *E.* n.sp. E Zones and is equivalent to Stage Lower 5b.

   f) The Lakes Road Rhyolite age of 274.1 ± 3.4 Ma lies within Lower Stage 4. The Formation is equivalent in age to the Greta Coal Measures that lie within the upper half of Lower Stage 4. This in turn is equivalent to the lower *E. preovalis* Zone.

   g) The Alum Rock Conglomerate ages averaged to a midpoint of 293 ma have *S. subcircularis* Zone above and *Trigonotreta*. sp. Zone below. These zones are equivalent to Stage 3a above and Stage 3a to Stage 2 below.

4. Boundaries between biostratigraphical zones are drawn based upon interpolation from known data using the criteria as follows:

   a) *Protohaploxypinus microcorpus* Zone is above the $\delta^{13}C$ negative excursion and the *Playfordiaspora crenulata* Zone is below (from Fig. 2.19). *Weylandites* Zone is below the $\delta^{13}C$ negative excursion (from Fig. 2.3 and Fig. 2.33).

   b) The Upper 5/ Lower 5 boundary is picked mid-way between data points Upper 5c/Lower 5b.

   c) The Stage 5/ Stage 4 boundary is picked 2/3 of the way above data Lower Stage 5/ Lower Stage 4 (upper half) to make space for the Upper Stage 4.

   d) The Stage 4/ Stage 3 boundary is picked 2/3 of the way above data Lower Stage 4/ Stage 3a to make space for Stage 3b.

   e) The Stage 3/ Stage 2 boundary is picked within the *Trigonotreta* n sp. Zone.

   f) The base of Stage 2 is assumed equivalent to the base of the Permian and taken to be at 300 Ma (Hess and Lippolt, 1986, p. 143).

5. Boundaries between formations are drawn based upon interpolation from linking back into biostratigraphy and interposition.

   a) The base Rewan/ top Bandana and the Narrabeen/ Newcastle Coal Measures are picked equivalent to the Permian-Triassic boundary from correlation to the negative $\delta^{13}C$ excursion at the paleontologically determined Permian-Triassic boundary in Meishan Section D, China.

b) The Black Alley Shale and the Shortland Formation are interpreted as the same age stratigraphically below the Bandana Coal Measures and the Newcastle Coal Measures.

c) The Peawaddy Formation and Dempsey formation are within *E. ovalis* Zone.

d) The Catherine Sandstone/ Ingelara/Freitag Formations are above the base of Upper Stage 5 and the Warranilla Formation is below the top of Lower Stage 5. The Four Mile Creek Formation is interposed between the Dempsey Formation and the Wallis Creek Formation which straddles the Upper Stage 5/ Lower Stage 5 boundary (Briggs, 1993, p. 289).

e) The upper Aldebaran Formation is interpreted as equivalent in age to the Mulbring Siltstone while the lower Aldebaran Formation is equivalent to the Lower Maitland Group by interpolation.

f) The Greta Coal Measures, Sydney Basin are equivalent to the Lakes Road Rhyolite and are Lower Stage 4.

g) The base of the Cattle Creek Formation/ Reids Dome Beds, Bowen Basin contains the Stage 4/ Stage 3b boundary and is equivalent to the Farley Formation/ Rutherford Formation.

h) The Joe Joe Beds, Galilee Basin contain the Stage 3a/Stage 2 boundary and is correlated to the Allandale Volcanics/ Lochinvar Formation, Sydney Basin.

6. Isotope stratigraphic ties to the Global Timescale.

a) The negative $\delta^{13}C$ excursion at the Permian-Triassic boundary is equivalent to the Griesbachian/ Changxingian boundary.

b) The $^{87}Sr/^{86}Sr$ minimum at the Guadalupian/ Ochoan boundary, 0.70672 in the Castile Formation (Denison et al., 1994, p. 162) not in the Salada Formation (Denison et al., 1994, p. 162) presumably at or near the base of the Ochoan and overlying the Lamar Member of the Bell Canyon Formation which is top Guadalupian and has a $^{87}Sr/^{86}Sr$ of 0.70682 (Denison et al., 1994). The $^{87}Sr/^{86}Sr$ minimum is found at the Peawaddy Formation/ Ingelara Formation boundary in Eddystone-5, Bowen Basin (Fig. 2.22). This $^{87}Sr/^{86}Sr$ minimum is equivalent to the Longtanian (=Djulfian)/ Capitanian (=Kazanian) Boundary (Harland et al., 1990, p. 48).

7. The Interpolation of the Global Time Scale.

a) The Changxingian base is assigned an age 3 million years down from the Permian-Triassic boundary identified by the negative carbon isotope excursion. The base of the Djulfian is identified by the $^{87}Sr/^{86}Sr$ minimum.

b) The Ingelara Formation/Peawaddy Formation with Kazanian foraminifera (Palmieri et al., 1994; Palmieri, 1990) is picked as topmost Kazanian (*Lunacammina maioris* Zone in Eddystone 5, Palmieri pers. com., 1992; Fig. 2.22) because the $^{87}Sr/^{86}Sr$ minimum occurs at the base Longtanian.

c) The Mulbring Formation is assigned a Ufimian age.

d) Stage 3b is assigned as Sterlitamakian and Stage 3a is Tastubian (Veevers, 1994b).

e) The Autunian/Stephanian boundary is dated as 300 Ma by Hess and Lippolt (1986).

f) The Asselian is interpositioned between the 300 Ma sample and the Tastubian. The Artinskian and Kungurian are interpositioned between the Sterlitamakian and Ufimian.

I adopt the Triassic timescale of Harland et al. (1990, fig. 3.8) with unchanged ages for the Late Triassic stages (Carnian 235 Ma, Norian 223 Ma, Rhaetian 210-208 Ma). The rest of the Triassic is recalibrated thus and shown in Figs 6.5.

a) The Permian-Triassic boundary is placed at 250 Ma, as in the Permian timescale.

b) The later part of the middle Anisian in North America with the bivalve *Daonella* is regarded as the same age as the *Daonella*-bearing tuff at the base of the New Zealand Etalian stage; biotite from the tuff is dated, by the $^{40}Ar/^{39}Ar$ plateau method, as 242.8± 0.6 Ma (Retallack et al., 1993). From this data point, Retallack et al. (1993) place the Scythian/ Anisian boundary at 246 Ma, and the Anisian/Ladinian boundary at 240.5 Ma. I arbitrarily subdivide the Scythian (or Early Triassic) epoch equally into its three stages (Griesbachian, Nammalian and Spathian), and place the boundary between the Smithian and Dienerian substages at 248.0 Ma. The conodont zones are from Ding (1992, p. 115) and Sweet et al. (1992, p. 2). The Western Australian dinocyst and palynological zonation is calibrated to the global timescale through conodont zones (Gorter 1994, p. 400; Nicoll and Foster 1994, fig. 4).

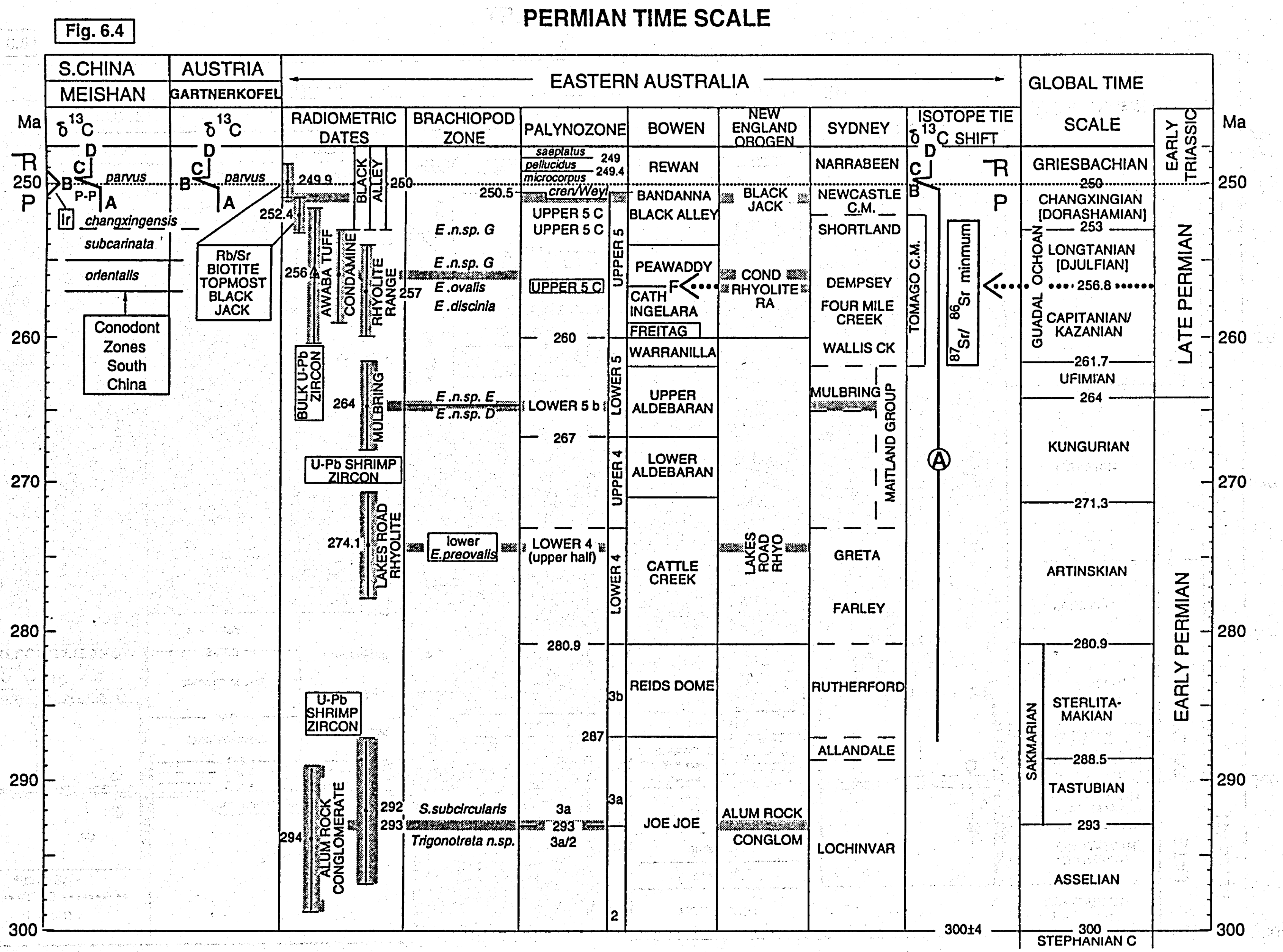

Figure. 6.4 The Australian Permian timescale.

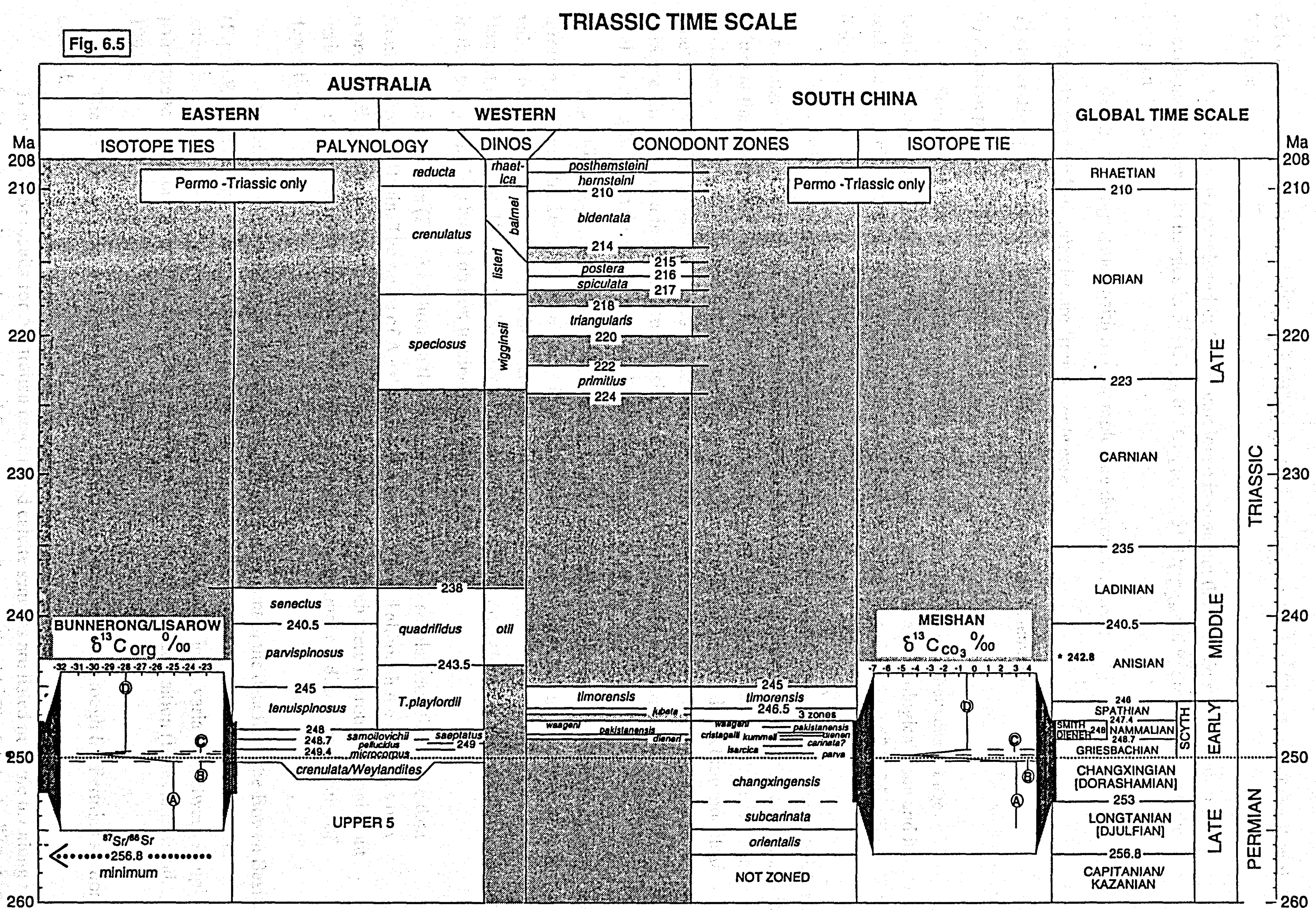

Figure. 6.5 The Australian Permian and Triassic timescale.

6.11 Composite profiles of $\delta^{13}C_{org}$, $\delta^{13}C_{CO3}$, Δ, $\delta^{18}O_{CO3}$, and $^{87}Sr/^{86}Sr$ through the Permian - Triassic

The timescale developed in 6.10 is employed in ordering the isotopic results against time to evaluate the secular changes in $\delta^{13}C_{org}$, $\delta^{13}C_{CO3}$, Δ, $\delta^{18}O_{CO3}$, and $^{87}Sr/^{86}Sr$ through the Permian -Triassic.

Relative stratigraphic positions of samples are determined from:

1) Sample depth where samples are from a single core.

2) Biostratigraphy based on palynological zones or associated faunal elements.

3) Relative position within a formation.

Sample ages are estimated by assuming a constant rate of deposition between set age markers in any single biostratigraphical zone such as the beginning of a palynological zone and its end. For example, a sample from the top Peawaddy Formation is assigned an age of 254 Ma (Fig. 6.4).

The $\delta^{13}C_{org}$ profile (Fig. 6.6) shows a clear distinction between values in the Permian which are less depleted in ^{13}C and those of the Triassic which are more depleted in ^{13}C. The negative excursion in values at the interpreted Permian-Triassic boundary is dramatic. Through the Permian there is a slight tendency for $\delta^{13}C_{org}$ values to become more negative though with the limited dataset it is not clear whether this is due to sampling bias as the samples in the lower Permian come predominantly from the Paradise Cores section in the Canning Basin. Compston (1960) reported a general decline in $\delta^{13}C_{org}$ in coal samples between the Early and Late Permian of around 2- 3‰.

The $\delta^{13}C_{CO3}$ profile (Fig. 6.7) from the Australian sections shows no apparent secular variation through the Permian. Data from the Early Triassic in this study are limited but are more negative than values from the Permian. The secular variations shown in the Permian $\delta^{13}C_{CO3}$ profile developed by Baud et al. (1989, fig. 18) using whole-rock limestones is not clearly developed in the Australian dataset in this study which is based on non luminescent brachiopod calcite.

The Δ profile (Fig. 6.8) through the Permian shows no clear secular variation in the data from the Bowen Basin. The range of Δ values is -26.8 to -32.5‰ and although the extremes may represent diagenetic alteration of either $\delta^{13}C_{CO3}$ or $\delta^{13}C_{org}$ or both there is probably significant variation between sample pairs due to variations in local environmental conditions at the time of deposition.

No clear secular variation in Δ through the Permian is evident in the data from the Bowen Basin (Fig. 6.8). The range of Δ is -26.8 to -32.5‰ and although the extremes may represent diagenetic alteration of either $\delta^{13}C_{CO3}$ or $\delta^{13}C_{org}$ or both there is probably significant variation between sample pairs due to variations in conditions in local environments at the time of deposition (Bates and Brand, 1991).

The $\delta^{18}O_{CO3}$ (Fig. 6.9) shows no clear evidence of a secular trend though the Permian section studied.

The $^{87}Sr/^{86}Sr$ results for Australian brachiopod calcite samples are listed in Table 6.7 along with an estimated age for each sample determined from the plot markers outlined in Fig.6.4. In the $^{87}Sr/^{86}Sr$ profile (Fig. 6.10) the late Early to Late Permian of the Bowen Basin is marked by fall in $^{87}Sr/^{86}Sr$ from about 0.70720 in sediments of palynological zone Lower Stage 4, interpreted as Artinskian stage, to a minimum of 0.70647 in lower Upper Stage 5 and thereafter by a rise in the $^{87}Sr/^{86}Sr$ profile that continues to the Cherrabun member of the Hardman Formation, Canning Basin. The dataset is insufficient to determine minor secular variations that might occur in the stratigraphic record however the dataset is consistent with the $^{87}Sr/^{86}Sr$ profiles of Popp et al. (1986b) and Denison et al. (1994). The location of the minimum $^{87}Sr/^{86}Sr$ value at or about the base of the Peawaddy Formation suggests a correlation of that stratigraphic level in Eastern Australia with the Guadalupian/Ochoan stage boundary in North America where a minimum in the $^{87}Sr/^{86}Sr$ profile is recorded (Denison et al., 1994).

6.12 Conclusion

Two global geochemical events are preserved in sediments from Australian sedimentary basins, the minimum in the $^{87}Sr/^{86}Sr$ profile and the negative $\delta^{13}C$ excursion. Identification of these events can be used to time calibrate Australian sedimentary basins of Permian-Triassic age.

The Permian-Triassic boundary as indicated by the $\delta^{13}C$ excursion occurs at or near the base of the *P. microcorpus* palynological zone in Australia. This indicates the Permian-Triassic boundary closely approximates the coal measures/ barren measures with red beds boundary in Eastern Australia as was traditionally proposed by David and Browne, (1950). This links a floral mass extinction as indicated by the *Falcisporites* Superzone (Helby et al., 1987) with the Permian-Triassic boundary (Retallack, 1995).

The secular variation in $\delta^{13}C$ values detected in carbonates in Tethys and South China at the Permian-Triassic boundary is present in organic matter from Australian marine and nonmarine sedimentary basins. The magnitude of the $\delta^{13}C$ excursion is generally between 5.5 and 10‰. Because this $\delta^{13}C$ excursion is present in both marine and nonmarine sediments the oxidation of a huge volume of ^{13}C-depleted carbon is interpreted to have occurred about the Permian-Triassic boundary. Such an event would have caused a greenhouse effect and global temperature rise. This greenhouse effect probably contributed significantly to the Permian-Triassic mass extinction.

The $^{87}Sr/^{86}Sr$ profile minimum does not occur at the Permian-Triassic boundary but precedes the boundary by several million years. The $^{87}Sr/^{86}Sr$ profile minimum may therefore be a signature of an event that led to a sequence of events which caused the Permian-Triassic mass extinction but cannot be directly linked with the end Permian extinctions.

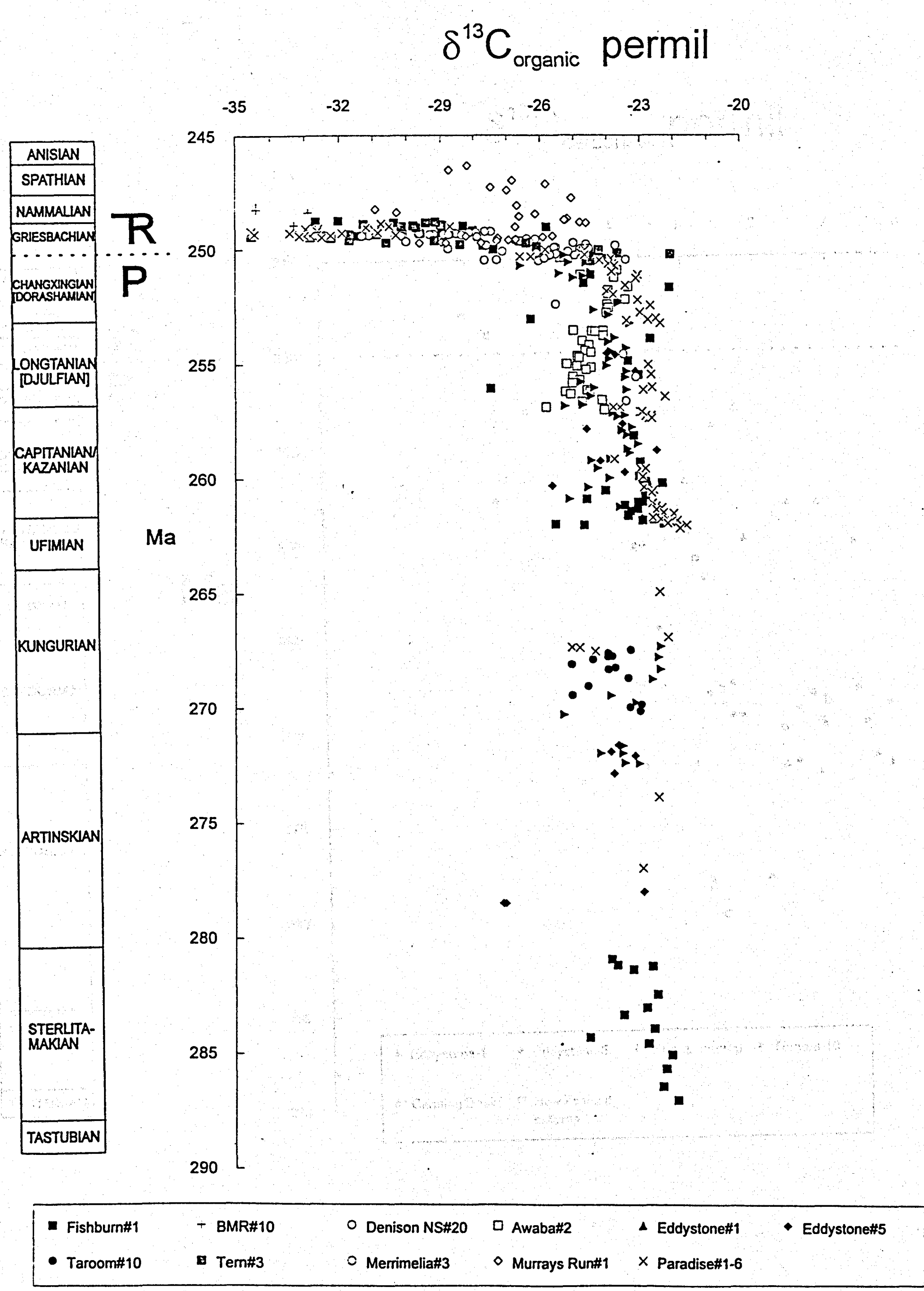

Fig. 6.6 $\delta^{13}C_{org}$ profile through the Permian-Triassic of Australia.

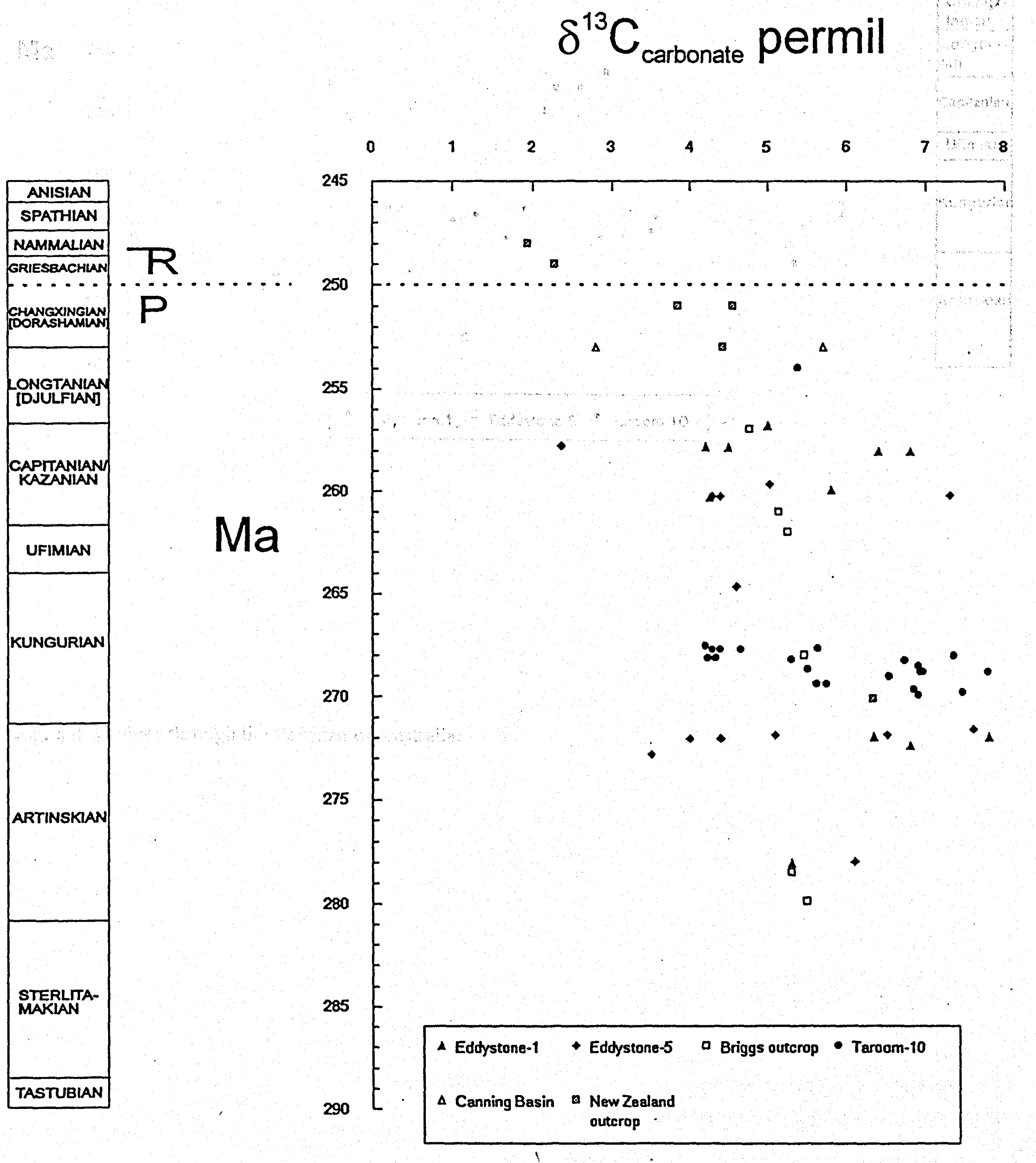

Fig. 6.7 $\delta^{13}C_{CO3}$ profile through the Permian-Triassic of Australia.

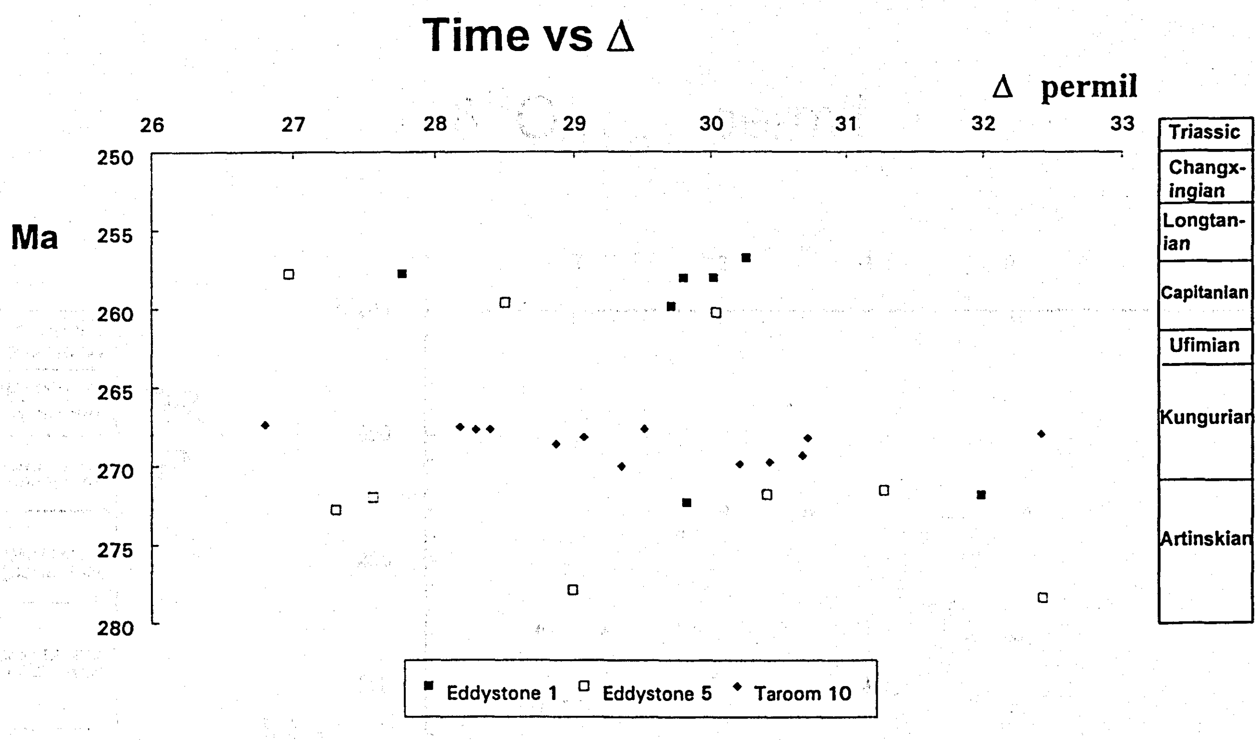

Fig. 6.8 Δ values through the Permian of Australia.

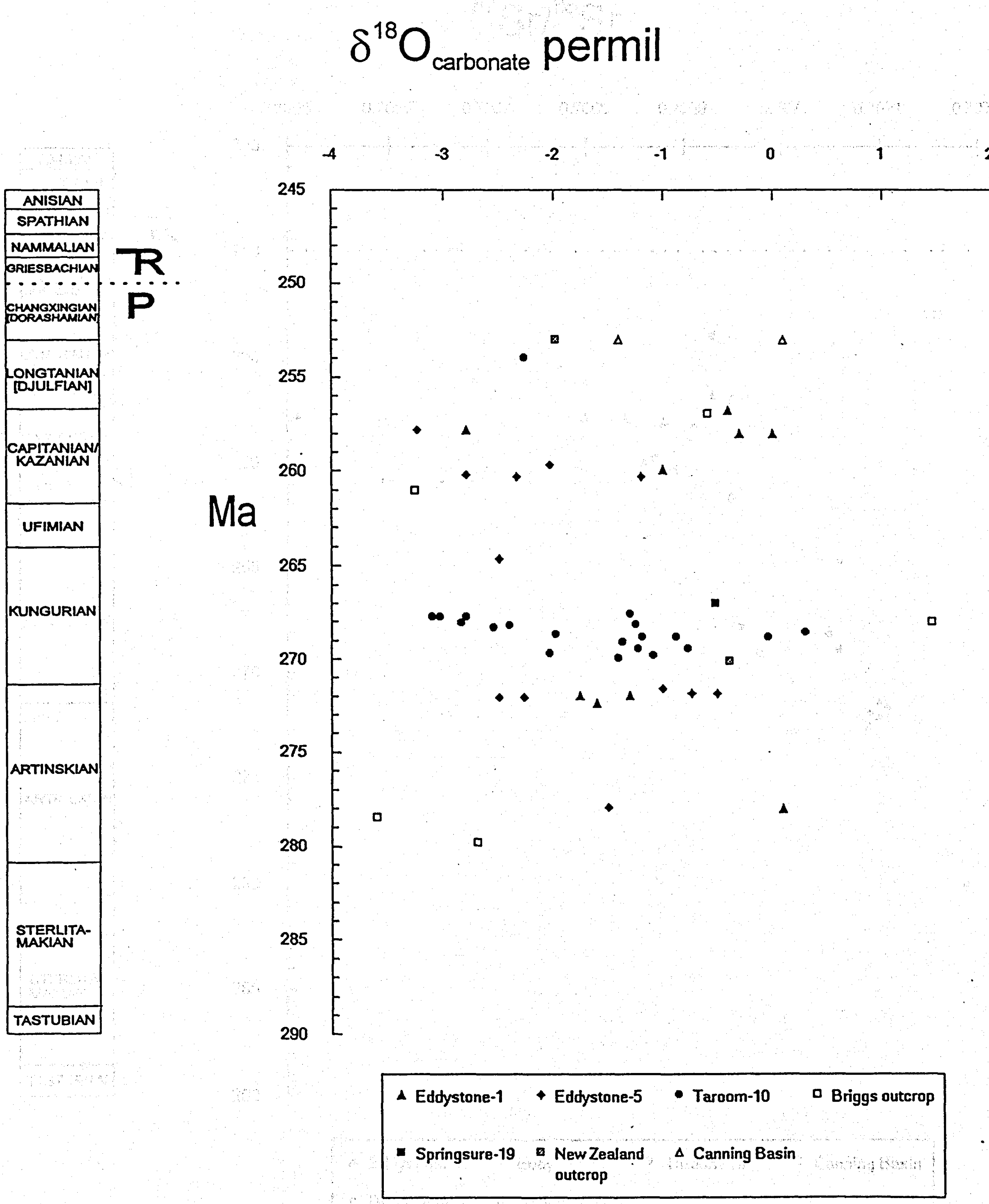

Fig. 6.9 $\delta^{18}O_{CO3}$ through the Permian-Triassic.

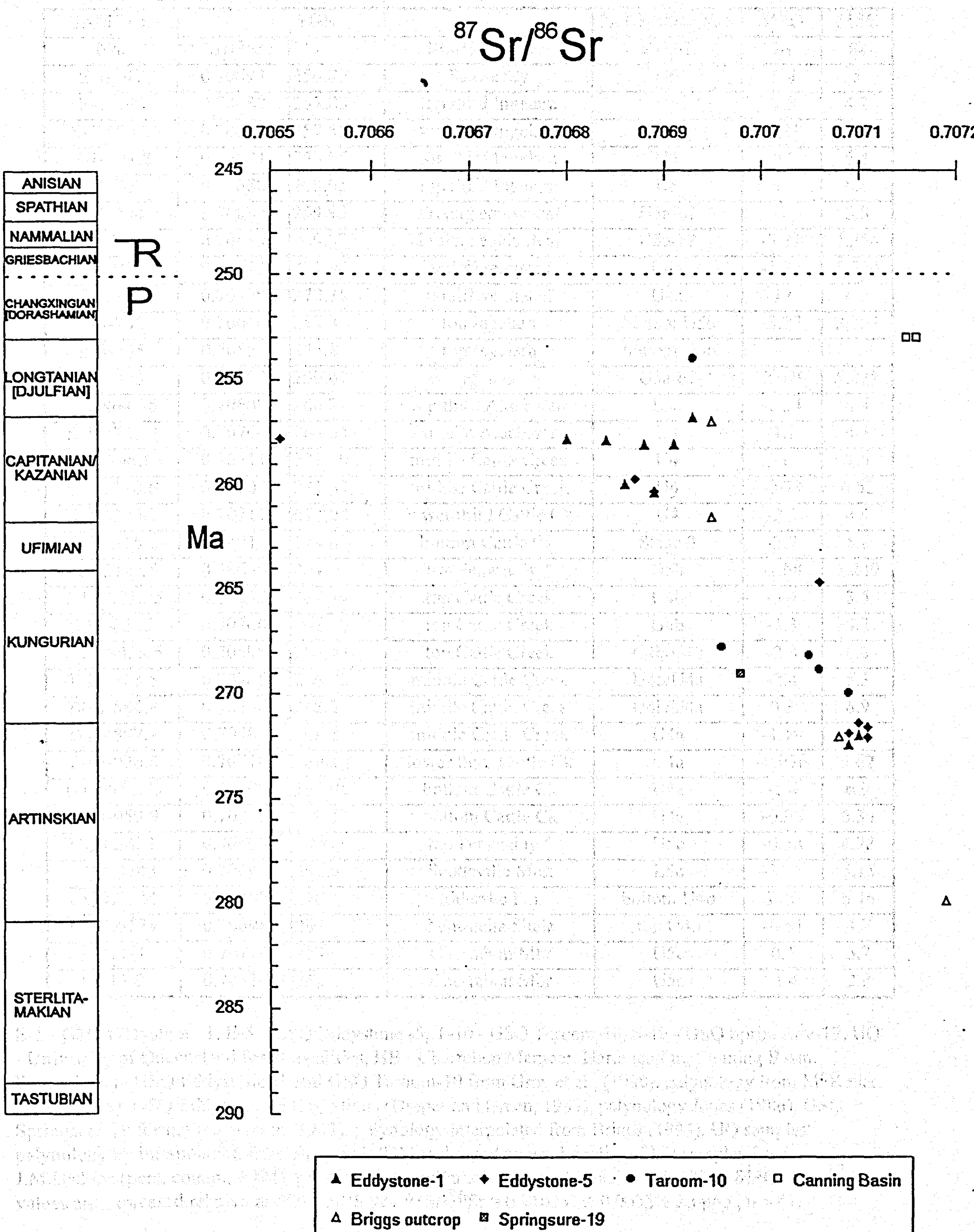

Fig. 6.10 $^{87}Sr/^{86}Sr$ profile through the Permian of Australia.

Table 6.8 Strontium isotope values in the Permian.

SAMPLE No.	$^{87}Sr/^{86}Sr$	AGE Ma	FORMATION	PALYNOLOGY ZONE	$\delta^{18}O$ ‰	$\delta^{13}C$ ‰
E-1-647	0.70693	256.79	Peawaddy	U5	-0.4	5
E-1-692	0.70680	257.83	top third Ingelara	U5	-2.8	4.2
E-1-693.8	0.70684	257.86	top third Ingelara	U5	-1.31	4.5
E-1-701.8	0.70691	258.05	top third Ingelara	U5	-0.3	6.4
E-1-702	0.70688	258.05	top third Ingelara	U5	0	6.8
E-1-784	0.70686	259.93	Freitag equivalent	U5a-b?	-1	5.8
E-1-793.1	0.70689	260.32	Freitag equivalent	U5a-b?	-3.31	4.254
E-1-937	0.70710	271.94	undifferentiated	U4a	-1.76	6.339
E-1-947	0.70709	272.38	undifferentiated	U4a	-1.6	6.8
E-5-735	0.70646	257.8	top Ingelara	bottom U5b	-3.27	2.357
E-5-735	0.70651	257.8	top Ingelara	bottom U5b		
E-5-833	0.70687	259.67	Freitag	U5a-b?	-2.029	5.032
E-5-864.35	0.70689	260.27	top third Aldebaran	L5c	-2.34	4.4
E-5-972.59	0.70706	264.64	middle Aldebaran	U4	-1.2	4.3
E-5-1196.84	0.70711	271.59	middle Cattle Creek	U4	-1	7.6
E-5-1210.6	0.70709	271.87	middle Cattle Creek	U4	-0.73	6.52
E-5-1219.3	0.70711	272.05	lower third Cattle Ck	U4	-2.5	4.4
E-5-1316.2	0.70719	279.83	bottom Cattle Ck.	Stage 3	-2.7	5.5
S19-514.25	0.70689	254	top Peawaddy *	U5b	-2.68	5.249
T-10-831.25	0.70693	267.44	top Cattle Creek	U4b	-3.4	3.5
T-10-838.2	0.70700	267.58	top Cattle Creek	U4b	-1.3	4.2
T-10-845.25	0.70696	267.73	top Cattle Creek	U4b/U4a	-2.8	4.3
T-10-868.8	0.70705	268.13	middle Cattle Creek	U4b/U4a	-2.4	5.3
T-10-884.4	0.70706	268.3	middle Cattle Creek	U4b/U4a	0.3	6.9
T-10-897.2	0.70706	268.8	middle Cattle Creek	U4a	-1.19	6.96
T-10-926.8	0.70710	269.42	lower third Cattle Ck	U4a	-0.076	5.62
T-10-952.39	0.70709	269.95	bottom Cattle Ck	U4a	-1.4	6.9
T-10-959.9	0.70713	270.1	bottom Cattle Ck	U4a	-0.96	6.33
UQ L2421	0.70695	254	top Peawaddy *	U5c	-0.58	4.78
UQ L3543	0.70695	261.5	Scottsville Mbr.	L5c	-3.26	5.15
UQ L5124	0.70708	270	Elderslie Fm.	bottom U4b	1.46	5.46
UQ L5129	0.70698	267	Fenestella Shale	top U4b	-0.51	4.7
HB11-1	0.70716	253	Cherrabun Mbr	U5c	0.1	5.7
HB11-2	0.70715	253	Cherrabun Mbr	U5c	-1.4	2.8

E-1 - GSQ Eddystone -1, E-5 - GSQ Eddystone -5, T-10 - GSQ Taroom-10, S-19 - GSQ Springsure-19, UQ - University of Queensland fossil localities, HB - Cherrabun Member, Hardman Fm, Canning Basin. Formations in GSQ Eddystone -1 and GSQ Taroom-10 from Gray et al., (1980), palynology from M^cKellar, (1977; 1978); GSQ Eddystone -5 formations (Draper and Green, 1983), palynology Jones (1986); GSQ Springsure-19 formations (Green, 1982), palynology interpolated from Briggs (1993). UQ samples' palynology by interpolation from Briggs (1993) brachiopod zones. Locality of HB samples from J.M.Dickins (pers. comm., 1994), palynology from Paradise Cores (Morante et al, 1994). $\delta^{13}C$ and $\delta^{18}O$ values are expressed relative to PDB. NBS 987 $^{87}Sr/^{86}Sr = 0.710257 \pm 0.0032\%$ 2σ pop., n = 41.